Performance Evaluation of Low-Complexity Multi-Cell Multi-User MIMO Systems

by

Jun Zhu
B.Eng., Southeast University, Nanjing, P.R.China, 2008

A Thesis Submitted in Partial Fulfillment of the
Requirements for the Degree of

MASTER OF APPLIED SCIENCE

in the Department of Electrical and Computer Engineering

Performance Evaluation of Low-Complexity Multi-Cell Multi-User MIMO Systems

by

Jun Zhu
B.Eng., Southeast University, Nanjing, P.R.China, 2008

Supervisory Committee

Dr. Hong-Chuan Yang, Supervisor
(Department of Electrical and Computer Engineering)

Dr. Lin Cai, Departmental Member
(Department of Electrical and Computer Engineering)

Dr. Kui Wu, Outside Member
(Department of Computer Science)

Supervisory Committee

Dr. Hong-Chuan Yang, Supervisor
(Department of Electrical and Computer Engineering)

Dr. Lin Cai, Departmental Member
(Department of Electrical and Computer Engineering)

Dr. Kui Wu, Outside Member
(Department of Computer Science)

ABSTRACT

The idea of utilizing multiple antennas (MIMO) has emerged as one of the significant breakthroughs in modern wireless communications. MIMO techniques can improve the spectral efficiency of wireless systems and provide significant throughput gains. As such, MIMO will be increasingly deployed in future wireless systems. On the other hand, in order to meet the increasing demand for high data rate multimedia wireless services, future wireless systems are evolving towards universal frequency reuse, where neighboring cells may utilize the same radio spectrum. As such, the performance of future wireless systems will be mainly limited by inter-cell interference (ICI). It has been shown that the throughput gains promised by conventional MIMO techniques degrade severely in multi-cell systems. This definitely attributes to the existence of the ICI.

A lot of related work has been performed on the ICI mitigation or cancellation strategies, in multi-cell MIMO systems. Most of them assume that the channel and even data information is available at the collaborating base stations (BSs). Different from the previous work, we are looking into certain low-complexity codebook-based multi-cell multi-user MIMO strategies. For most of our work, we derive the statistics of the selected user's signal-to-interference-and-noise-ratio (SINR), which enable us to calculate the achieved sum-rate accurately and efficiently. With the derived sum-rate

expressions, we evaluate and compare the sum-rate performance for several proposed low-complexity ICI-mitigation systems with various system parameters for single-user per-cell scheduling case.

Furthermore, in order to fully exploit spatial multiplexing gain, we are considering multi-user per-cell scheduling case. Based on the assumption that all CSI including intra-cell and inter-cell channels are available at each BS, we firstly look into the centralized optimization approach. Typically, since the sum-rate maximization problem is mostly non-convex, it is generally difficult to obtain the globally optimum solution. Through certain approximation and relaxations, we successfully investigate an iterative optimization algorithm which exploits the second-order cone programming (SOCP) approach. From the simulation results, we will observe that the iterative option can provide near-optimum sum capacity, although only locally optimized. Afterwards, inspired by the successful application of Per-User Unitary Rate Control (PU^2RC) scheme, we manage to extend it into dual-cell environment, with limited coordination between two cells.

Contents

List of Figures

ACKNOWLEDGEMENTS

I would like to thank:

Dr. Hong-Chuan Yang, for his support and guidance during my master study, which have made this thesis possible. I thank him for his insights and suggestions that helped to shape my research skills. His valuable feedback contributed greatly to this thesis.

Dr. Lin Cai, and Dr. Kui Wu, for their valuable feedback which helped me to improve the thesis in many ways.

Dr. Andreas Antoniou, Dr. Xiao-Dai Dong and Dr. Wu-Sheng Lu, for their guidance and help through graduate courses, which have equipped me with solid foundation in theory, practice and prepared me for further study and research.

My dear laboratory colleagues and friends in Victoria, for their presences and fun-loving spirits that made the otherwise grueling experience enjoyable. They are Dr. Peng Lu, Nan Lv, Lei Zhang, Dong Zhang, Yingduo Chen, Yimian Du, Liya Zhu, Dr. Wei Xu, Ning Wang, Shaochen Qu, Bojiang Ma, Wenhao Jin, Jie Yan, and Ji Huang.

My grandma and parents, for always being there when I needed them most, and for supporting me through all these years.

I believe I know the only cure, which is to make one's centre of life inside of one's self, not selfishly or excludingly, but with a kind of unassailable serenity-to decorate one's inner house so richly that one is content there, glad to welcome any one who wants to come and stay, but happy all the same in the hours when one is inevitably alone.

Edith Wharton

Chapter 1

Introduction

Multi-input-multi-output (MIMO) wireless systems can achieve impressive spectral efficiency improvements and provide significant throughput gains. With its potential to provide the next great leap forward in wireless evolution, MIMO has become the frontier of wireless communication research. For instance, it has been included in various wireless standards, such as UMTS (e.g., 3GPP), IEEE 802.11 (for wireless LANs) and proposals for next generation (4G and beyond) wireless systems. This chapter provides an overview of the fundamentals of multi-antenna systems, including multi-user MIMO systems, beamforming, limited feedback and multi-cell MIMO systems.

1.1 Multi-User MIMO Systems

In a standard point-to-point MIMO system, as illustrated in Fig. 1.1, the transmitter is equipped with N_t antennas, whereas the receiver equipped with N_r antennas.

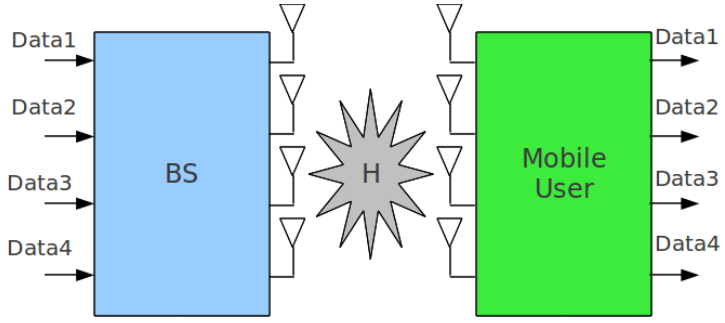

Figure 1.1: Point-to-point MIMO system model

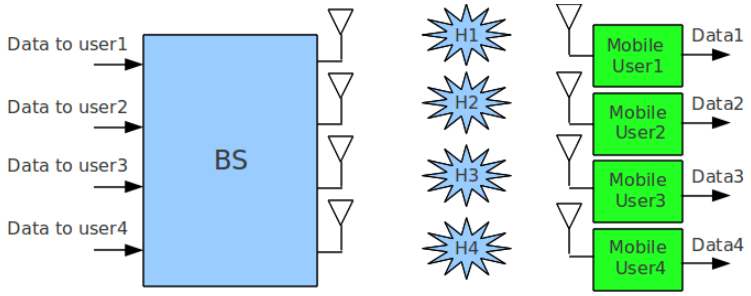

Figure 1.2: Multi-user MIMO system model

The capacity of the MIMO channel increases linearly with $\min\{N_t, N_r\}$, thanks to the diversity gain and multiplexing gain [1]-[3]. However, when deployed in cellular systems, due to size, cost and complexity restrictions, there is usually less or even single antenna at mobile user ends. Meanwhile, there are totally K active users in the system, and usually, $K > N_t$. Therefore, in order to fully exploit the spatial multiplexing gain [4], multiuser diversity gain [2] and improve the system throughput, the BS will transmit signals to multiple non-cooperative mobile users simultaneously. This resulting system is regarded as multi-user MIMO system, or downlink/broadcast MIMO systems.

In a multi-user MIMO system shown as in Fig. 1.2, the BS deployed with N antennas, transmits signals to totally N non-cooperative mobile users at the same time. Notice that simultaneously transmitting independent data streams will incur inter-user (or multi-user) interference, owing to the fact that a certain user is unable to distinguish its own desired signal and interference signals for other users. Thus, one of the toughest task for multi-user MIMO system is the multi-user interference mitigation. Based on the availability of channel state information (CSI) of mobile users at the BS, related studies have demonstrated to what extents the multi-user interference can be suppressed or mitigated. If assuming perfect CSI is available at the BS, information theoretical results have shown that spatial multiplexing gain can be fully exploited through multiple transmit antennas.

1.1.1 Capacity of MIMO broadcast channels

The capacity of the MIMO broadcast channels have already been well-understood according to related literature. Caire and Shamai in [5] have obtained the sum capacity of the MIMO broadcast channel for the special case of $K = 2$ users. They propose a transmission scheme applying Costas dirty paper coding (DPC) [6] and verify that

the scheme is optimal in achieving the sum capacity for two-user case, but requiring high computational complexity. Their work have then been generalized. Typically, the sum capacity for general cases under power constraints has been found in [7] through using a generalized decision feedback equalizer structure for precoding at the transmitter. According to [8], Vishwanath, Jindal and Goldsmith establish a duality between dirty paper region for the MIMO broadcast channel and capacity region of the MIMO access channel, which simplifies the calculation of the achievable region of the MIMO broadcast channel.

1.1.2 Beamforming techniques

The DPC [6] can achieve optimal sum capacity of MIMO broadcast channels, however, requiring non-linear processing and high computational complexity, which prohibits its implementation in practical systems. A lot of work has been focusing on low-complexity transmission that can effectively explore spatial multiplexing gain for MIMO broadcast channels. Among them, transmit beamforming is one of the suboptimal strategies that can serve multiple users simultaneously [9]. The data throughput achieved with beamforming is shown to scale at the same rate of $N \log\log(K)$ as DPC, when K is sufficiently large.

With transmit beamforming, the data stream of each selected user is coded independently and multiplied by a beamforming vector. The transmit vector is generated as the superposition of all selected users' data streams. Since the number of active users is usually larger than the number of transmit antennas, namely $K > N$, the BS may select a subset of users ($\leq N$) out of totally K users for simultaneous transmission. When users' channels experience independent fading, there is likely to be a subset of users with very good channel quality, which is characterized by more closeness to orthogonality between users' channel vectors and larger power gain. The sum rate, defined as the sum of data rates of all users, can be increased by transmitting to the specifically selected users. The system performance improvement brought by the spatial freedom is called multiuser diversity gain.

Beamforming vector design and use selection are the two crucial issues for transmit beamforming, which require certain forms of CSI from mobile users. Due to the loss of propagation channel reciprocity, frequency-devision-duplex (FDD) systems needs the CSI feedback from mobile users. Since feedback decreases spectral efficiency of wireless communications systems, there exists a tradeoff between feedback load and

sum-rate performance of multiuser MIMO systems. Current research interests focus on two low-complexity beamforming schemes, zero-forcing beamforming (ZFBF) [10] and random unitary beamforming (RUB) [11]. Both beamforming schemes are shown to achieve the same scaling law as DPC when there are asymptotically large number of users in the system.

1.1.3 Limited feedback techniques

It is known that in FDD systems, full-CSI feedback is required, which is infeasible in practical multi-user systems. The number of feedback bits can be substantially reduced by predefining a set of beamforming vectors, i.e. a beamforming codebook, known at both the BS and the user ends. Once the receiver chooses the optimal beamforming vector from the codebook as a function of CSI, only the index of this beamformer needs to be sent to the BS. Various codebook construction methods for MIMO and MISO channels together with the corresponding codeword selections have thus far been developed [12]. It is noticeable that most of the work in this thesis relies on the codebook-based limited feedback techniques. And for analytical tractability and consistency, only randomly generated codebook is considered here.

1.1.4 PU^{2}RC- a practical multi-user MIMO system implementation

Per-User Unitary Rate Control (PU^{2}RC) [13] is the advanced multi-user MIMO technique which utilizes the concept of transmit beamforming, limited feedback and scheduling to enhance the system performance of multiple antenna wireless networks. Users to be served are selected from the set of service-requesting users by the BS using the information provided by users. Data transmitted to mobile users are multiplied by a precoding matrix selected from the set of predefined matrices before transmission. The selection of users and the precoding matrix enables the utilization of multi-user diversity and reduces feedback overhead from users to the BS. Precoding matrices used in this scheme is unitary. The use of unitary precoding matrices facilitates the estimation of interference from other users' data to the unintended user. Inspired by its successful application, we manage to extend it into dual-cell environment, with limited coordination between two cells.

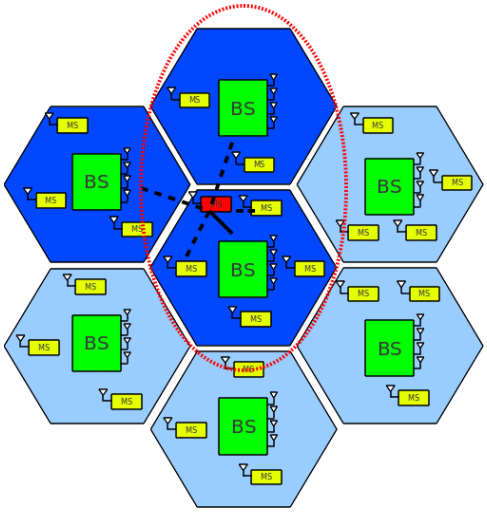

Figure 1.3: Multi-cell MIMO system model

1.2 Multi-Cell MIMO Systems

As described above, multiple-input multiple-output (MIMO) techniques can provide order of magnitude spectral efficiency improvements to wireless systems and achieved significant throughput gains for point-to-point communication and single-cell multi-user systems. Thus, MIMO has been identified as a key technology for future wireless broadband systems. On the other hand, in order to meet the increasing demand for high data rate multimedia wireless services, future wireless systems are evolving towards universal frequency reuse, where neighboring cells may utilize the same radio spectrum. As such, the performance of future wireless systems will be mainly limited by inter-cell interference [14]. It has been shown that the throughput gains promised by conventional MIMO techniques shrink severely in multi-cell systems [14]-[16], which primarily attributes to the existence of the inter-cell interference (ICI). Therefore, the effective ICI mitigation or cancellation strategies, and multi-cell MIMO transmission have drawn significant research attention recently [17]-[20].

The system model of multi-cell MIMO system is depicted in Fig. 1.3. All the ICI suppression and multi-cell processing techniques require the information sharing between participating BSs. Either channel state information (CSI) or data information (DI) or both might be shared [23]. If both CSI and DI are fully shared between BSs, the coordinated BSs effectively constitute a 'super-BS', which transforms several interfering channels into a single MIMO broadcast channel. Conventional MIMO broadcast transmission with individual power constraints on each BS can be applied

[24] [28]. The optimal dirty paper coding (DPC) [6] and sub-optimal linear precoders have been studied for network MIMO scenario [18]-[21]. These coordination strategies usually require huge load of overhead signaling [22]. Note that, although BSs are usually connected with wired connections with each other through the switching center, these connections are already fully loaded with the increasing amount of multimedia data traffics.

Certain partial or no information sharing strategies are also under investigation. Beamforming vectors or precoding matrices are jointly designed such that the intended signals are orthogonal to the interference channels [25] [26]. Typically, still in [26], an adaptive strategy was proposed which cancels inter-cell interference between scheduled user using joint beamforming only when the interference is significant. [23] has proposed random beamforming strategies to 3GPP where two BSs share much less. In this case, the interference is mitigated through coordination. And exact sum-rate performance analysis of the specific dual-cell system is presented in our previous work [27].

1.3 Contribution and Significance of Work

Most of the related work described above are based on the fundamental assumption that the channel and data information is available at the BS, and most results have been derived through Monte-Carlo simulations. In this thesis, we study the low-complexity beamforming schemes through accurate theoretical analysis. This approach serves two purposes. The first is to provide an exact expression of the sum capacity, based on which we can study the relation between sum capacity and various system parameters including the number of transmit antennas, the number of active users, feedback load, and average channel SNR. The second is to optimize design parameters in user selection/scheduling to maximize sum capacity.

Based on the theoretical results, various strategies have been proposed under the dual-cell or two-tier femtocell scenario, so that inter-cell interference has been mitigated. The main contributions include: 1) In the dual-cell system, we consider three user selection schemes that exchange no or limited amount of control information to achieve coordinated beamforming, and then accurately quantify their performance through statistical analysis. Both non-orthogonal and orthogonal codebook are under consideration. 2)In the two-tier femtocell system, we consider two schemes that exchange a small amount of control information to achieve coordinated beamforming.

We evaluate the performance of the resulting system in terms of system throughput through accurate mathematical analysis and compare them with other design options.

All the work described above share the limitation of single-user per-cell scheduling, which does not fully exploits spatial multiplexing gain. Thus, multi-user per-cell scheduling is also under study, and certain successful results have already been investigated. An iterative optimization algorithm has been discovered, which exploits the second-order cone programming (SOCP) approaches, so as to provide an optimal performance for dual-cell transmission. A more practical multi-user scheduling scheme is introduced and discussed afterwards, with only certain beam index sharing between two cells.

It is also worth noting that although most of the work in this thesis are based on two cells, all the strategies can be extended into multi-cells directly and smoothly. We consider the dual-cell case only for the sake of analytical consistency and tractability.

1.4 Thesis Outline

The rest of the thesis are organized as follows. Chapter 2 considers three low-complexity approaches for dual-cell random beamforming transmission. In Chapter 3, we present the sum rate analysis of dual-cell system with coordinated unitary beamforming. Chapter 4 will look into multi-user scheduling per-cell for dual-cell transmission. Afterwards, two coordinated beamforming approaches have been discussed for two-tier femtocell networks in Chapter 5. Certain conclusions and future work are discussed in Chapter 6.

Chapter 2

Dual-Cell Random Beamforming Transmission

With conventional network-MIMO approach, multiple coordinated BSs effectively constitute a 'super-BS', which transforms several interfering channels into a MIMO broadcast channel [24]-[29]. The optimal dirty paper coding (DPC) [6] and sub-optimal linear precoders have been studied for network MIMO scenario [18]-[21]. With some simplified network models, analytical results have appeared in [33]-[35]. These coordination strategies require, however, the complete channel state information, and, sometimes, even the user data to be shared among coordinating BSs, which introduce huge load of overhead signaling [22]. Note that, although BSs are usually connected with wired connections with each other through the switching center, these connections are already fully loaded with the increasing amount of multimedia data traffics. Recently, an adaptive strategy was proposed which cancels inter-cell interference between scheduled user using joint beamforming only when the interference was significant [26]. But user selection was not considered there.

Unlike previous works in the literature, we focus on more practical coordinated beamforming transmission schemes for dual-cell MIMO systems based on random beamforming in this chapter. For MIMO systems with random beamforming, in order to achieve good performance, proper user selection is essential. That also applies to coordinated beamforming transmission. To limit the amount of overhead signal between BSs and minimize the additional burden to the back haul connections, we consider the user selection schemes that exchange no or limited amount of control information to achieve coordinated beamforming. Specifically, we present and

study selfish random beamforming (SRB), interference-aware random beamforming (IA-RB), both of which require no information exchange between cells, and random beamforming with limited coordination (LC-RB), where only the selected beam index is shared among BSs. We would like to point out that some of these schemes have already been discussed in certain standard activities, such as 3GPP framework [36]. Our contribution is to accurately quantify their performance through statistical analysis. We firstly derive the exact analytical expression for the sum rate of the resulting systems assuming that all the users are located along the cell boundary and average inter-cell interference power at mobile users can be considered approximately identical. Selected numerical examples show that LC-RB can offer significant sum-rate capacity gain with low system complexity. During the sum rate performance analysis, we develop the exact statistics of users' SINRs based on some new statistic results of projection norm squares, which can be broadly applied into the performance analysis of other related systems.

We then extend the study to the more practical scenario, where the users are randomly distributed within the whole cell and average inter-cell interference power can no longer be regarded as identical, due to the different distances from the neighboring BS to the users. In this case, we propose an adaptive coordinated beamforming scheme and evaluate its performance and complexity. Specifically, the BS can decide whether to perform LC-RB to mitigate the inter-cell interference, or just to perform SRB, based on the distance information gathered from the mobile users. Note that our scheme differs from the adaptive scheme in [26] in that we consider user selection in each cell. Selected numerical examples show that LC-RB can offer significant sum-rate capacity gain with low system complexity.

The rest of the chapter is organized as follows. In Section 2.1, the system and channel models are introduced. Section 2.2 presents the proposed transmission strategies. The sum-rate performance analysis of the proposed systems is given in Section 2.3 (for identical interference power case) and in Section 2.4 (for non-identical interference power case). In Section 2.5, we investigate the adaptive implementation strategy for the general case. The chapter concludes in Section 2.6.

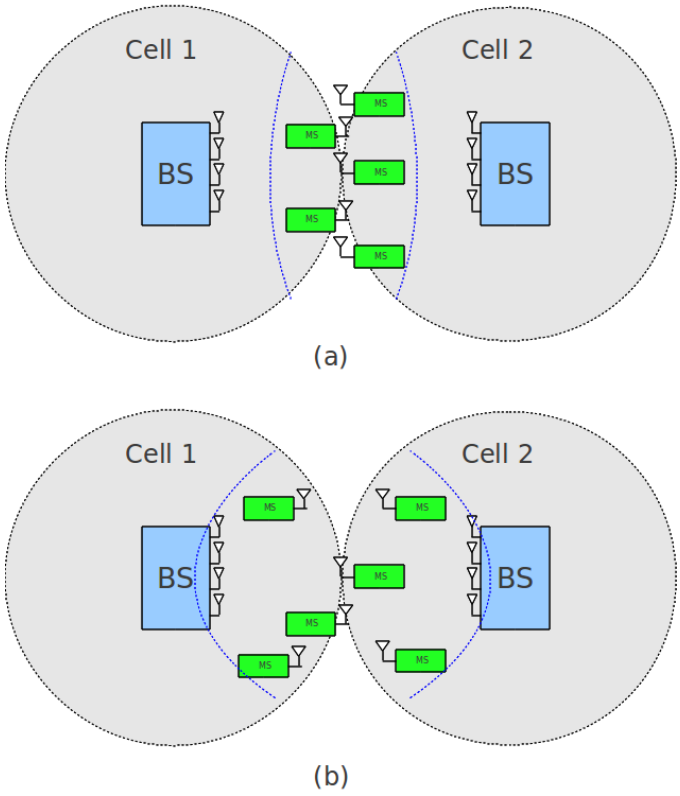

Figure 2.1: System model

2.1 System and Channel Models

The system under consideration as shown in Fig. 2.1 consists two base stations, utilizing the same radio spectrum to serve their selected users [1]. Both base stations are equipped with N antennas, which facilitates beamforming transmission, whereas each user has only a single receive antenna due to its size or complexity constraint. The user set in cell 1 is denoted by $\mathcal{I} = \{1, 2, \ldots, i, \ldots, K_1\}$, and that in cell 2 by $\mathcal{J} = \{1, 2, \ldots, j, \ldots, K_2\}$. The channel vectors are defined as following,

- $\mathbf{h}_{1i}$ is the $N \times 1$ channel vector from the base station 1 to the ith user in cell 1, i.e. $i \in \mathcal{I}$.
- $\mathbf{h}_{2i}$ is the $N \times 1$ channel vector from the base station 2 to the ith user in cell 1, i.e. $i \in \mathcal{I}$.
- $\mathbf{h}_{1j}$ is the $N \times 1$ channel vector from the base station 1 to the jth user in cell 2, i.e. $j \in \mathcal{J}$.
- $\mathbf{h}_{2j}$ is the $N \times 1$ channel vector from the base station 2 to the jth user in cell 2, i.e. $j \in \mathcal{J}$.

We assume that, with proper power control mechanism, the users experience homogeneous Rayleigh fading with respect to their target BS. Thus, each component of $\mathbf{h}_{1i}$ and $\mathbf{h}_{2j}$ is modeled as independent and identically distributed (i.i.d) complex Gaussian random variables with zero mean and unit variance. When mobile users are randomly populated in their specific cell coverage area, the average received interference power is dynamic, due to the various distances from the neighboring BS to the users. Each component of the interference channel vector, $\mathbf{h}_{1j}$ and $\mathbf{h}_{2i}$ is modeled as independent complex Gaussian random variables with zero mean and variance δ_j (resp. δ_i) with respect to user j (resp. i). As will be seen in later section, we will focus mostly on the interference channel from BS_2 to the selected user in cell 1, denoted by $\mathbf{h}_{2i^*}$. We assume that each component of $\mathbf{h}_{2i^*}$ is modeled as i.i.d. complex Gaussian random variables with zero mean and a common variance δ_{i^*}. For the special case that the mobile users are distributed along the cell boundary, and thus all the users have approximately the same distance with the neighboring BS, we can assume each component of $\mathbf{h}_{1j}$ and $\mathbf{h}_{2i}$ is modeled as i.i.d. complex Gaussian random variable with zero mean and variance δ, i.e. $\delta_i = \delta_j = \delta$ for all i and j.

[1] The system model is applied in Chapter 2, 3 and 4

We assume that each base station employs a codebook-based random beamforming strategy to serve one selected user in its coverage area. [2] The codebook is assumed to consist of B unit-norm vectors of length N, randomly generated from an isotropic distribution [51]. With their wired connection to the switching center, the BSs can exchange a limited amount of control information for coordinated beamforming transmission. Specifically, the BS can communicate the utilized beamforming vectors to each other and to the users using the index of the codebook. With the proper design of the beamforming vectors and user selection, the inter-cell interference can be controlled. The specific design and selection scheme proposed in this work will be discussed in the following sections. For the multi-transmit antenna case under consideration, the received signal at the ith user in cell 1 and jth user in cell 2 can be written as:

$$\begin{aligned} y_i &= \mathbf{h}_{1i}^T \mathbf{w}_1 s_1 + \mathbf{h}_{2i}^T \mathbf{w}_2 s_2 + n_i, i \in \mathcal{I}, \\ y_j &= \mathbf{h}_{2j}^T \mathbf{w}_2 s_2 + \mathbf{h}_{1j}^T \mathbf{w}_1 s_1 + n_j, j \in \mathcal{J}. \end{aligned} \tag{2.1}$$

respectively, where $s_i (i = 1, 2)$ are data symbols to selected users and $\mathbf{w}_i (i = 1, 2)$ are the corresponding beamforming vectors, n_i and n_j are the additive Gaussian noise.

2.2 Transmission Strategies

In this section, we present the fundamental principles and the mode of operations of several reduced-complexity dual-cell beamforming transmission strategies. For analytical tractability, we focus on dual-cell scenario.

2.2.1 Selfish random beamforming (SRB)

This scheme assumes that the system is completely unaware of the inter-cell interference. BS_1 and BS_2 just perform the conventional random beamforming separately. BS_1 (resp. BS_2) randomly selects a vector, denoted by $\mathbf{w}_1$ (resp. $\mathbf{w}_2$) from its codebook as beamforming vector and transmits a pilot symbol with this vector. Every user in the coverage area of BS_1 (resp. BS_2) will estimate and feed back its received signal to noise ratio (SNR), which will be proportional to the projection power of

[2] Other codebook such as Grassmannian codebook, may lead to better performance, but for analytical tractability, we limit ourself to random codebook

users channel vector on to the beamforming direction, i.e. $|\mathbf{h}_{1i}^T\mathbf{w}_1|^2$ (resp. $|\mathbf{h}_{2j}^T\mathbf{w}_2|^2$). Note that users will not need to estimate its channel vector in this process and each only needs to feed back a real number for user selection. BS_1 (resp. BS_2) will select the user achieving the largest SNR among all users, i.e. user i^* (resp. j^*), where $i^* = \arg\max_i |\mathbf{h}_{1i}^T\mathbf{w}_1|^2$ (resp. $j^* = \arg\max_j |\mathbf{h}_{2j}^T\mathbf{w}_2|^2$). With conventional random beamforming strategy, transmission will then start without any mechanism for controlling the interference from the other base station. Therefore, we can determine the SINRs of the selected users as

$$\gamma_1 = \frac{\max_i |\mathbf{h}_{1i}^T\mathbf{w}_1|^2}{|\mathbf{h}_{2i^*}^T\mathbf{w}_2|^2 + \rho}, \gamma_2 = \frac{\max_j |\mathbf{h}_{2j}^T\mathbf{w}_2|^2}{|\mathbf{h}_{1j^*}^T\mathbf{w}_1|^2 + \rho}, \tag{2.2}$$

where ρ is the normalized noise power, equal to N_0/E_s.

2.2.2 Interference-aware random beamforming (IA-RB)

The operations of this scheme shares a lot in common with the SRB scheme. The only difference is that, every user in the coverage area of BS_2 (BS_1 would follow exactly the same operations) will estimate and feed back its received signal to noise and interference ratio (SINR), with signal power proportional to $|\mathbf{h}_{2j}^T\mathbf{w}_2|^2$ and interference power to $|\mathbf{h}_{1j}^T\mathbf{w}_1|^2$. Specifically, the SINR of the jth user in the BS_2's coverage is given by

$$\gamma_{2,j} = \frac{|\mathbf{h}_{2j}^T\mathbf{w}_2|^2}{|\mathbf{h}_{1j}^T\mathbf{w}_1|^2 + \rho}. \tag{2.3}$$

Then, the BSs will select the user that achieves the largest SINR. Note that as long as the two BSs do not transmit their pilot symbols simultaneously, the users will not need to estimate their channel vectors to determine SINR. Again each user will only feed back a real number for user selection. And the achieved SINRs of the two selected users can be presented as

$$\gamma_1 = \max_i \left(\frac{|\mathbf{h}_{1i}^T\mathbf{w}_1|^2}{|\mathbf{h}_{2i}^T\mathbf{w}_2|^2 + \rho} \right), \gamma_2 = \max_j \left(\frac{|\mathbf{h}_{2j}^T\mathbf{w}_2|^2}{|\mathbf{h}_{1j}^T\mathbf{w}_1|^2 + \rho} \right). \tag{2.4}$$

2.2.3 Random beamforming with limited coordination (LC-RB)

The scheme differs from SRB and IA-RB as it achieves coordinated beamforming transmission with limited overhead signaling. Without loss of generality, we assume that BS_1 starts its user selection for beamforming transmission first. In particular, BS_1 performs exactly the same as SRB to complete the beam and user selection for first cell.

The selected user by BS_1, referred as user i^*, will estimate its MISO channel from the interfering base station BS_2, denoted by $\mathbf{h}_{2i^*}$. With this channel state information, user i^* will determine the beamforming vector that leads to the smallest amount of interference to itself and should be used by BS_2, and feed its index back. Mathematically speaking, the beamforming vector $\mathbf{w}_2$ should satisfy $|\mathbf{h}_{2i^*}^T\mathbf{w}_2|^2 = \min_l |\mathbf{h}_{2i^*}^T\mathbf{w}_l|^2$.

BS_1 will inform BS_2 the desired beamforming vector to use through the wired backhaul connection. BS_2 will broadcast training symbol using the selected beamforming vector for its own user selection. Every user in the coverage area of BS_2 will estimate and feedback its received SINR. BS_2 will select the user that achieves the maximum SINR among all users to serve, i.e. user j^* where $j^* = \arg\max_j \gamma_{2,j}$.

Based on the above mode of operation, we can determine the SINRs of the selected users with LC-RB, as

$$\gamma_1 = \frac{\max_i |\mathbf{h}_{1i}^T\mathbf{w}_1|^2}{\min_l |\mathbf{h}_{2i^*}^T\mathbf{w}_l|^2 + \rho}, \gamma_2 = \max_j \left(\frac{|\mathbf{h}_{2j}^T\mathbf{w}_2|^2}{|\mathbf{h}_{1j}^T\mathbf{w}_1|^2 + \rho} \right). \tag{2.5}$$

It is worth noting that the similar design have been considered in the standard activities for LTE Advanced and IEEE 802.16m [23]. In this work, we complement those simulation studies of such designs with the exact sum-rate capacity analysis.

2.3 Sum-rate Analysis for Identical Average Interference Power Case

This section provides the sum-rate analysis assuming that the average interference power is identically distributed, i.e. $\delta_i = \delta_j = \delta$. Essentially, we consider the scenario that mobile users are distributed along the cell boundary.

2.3.1 Common analysis

We first present some statistical results on the ordered projection norm squares, which will be broadly applied in the later analysis. Noting that each component of vectors discussed in this section is modeled as i.i.d. complex Gaussian random variable with zero mean and unit variance.

Let's firstly consider the projection norm squares of K independent vectors $\mathbf{h}_i, i = 1, ..., K$ to a normalized vector $\mathbf{w}$, i.e. $a_i \doteq |\mathbf{h}_i^T\mathbf{w}|^2, i = 1, 2, ..., K$. Since $\mathbf{h}_i$ are independent, and a_i are i.i.d. chi-square random variable with two degrees of freedom [52]. It follows that the probability density function (PDF) of the lth largest among totally K projection norm square $a_{l:K} = rank_l\{a_i\}, i = 1, 2, ..., K$ is given, after applying the basic ordered statistic result, by:

$$f_{a_{l:K}}(x) = \frac{K!}{(K-l)!(l-1)!}(1-e^{-x})^{K-l}e^{-lx}, x \geq 0. \tag{2.6}$$

We now consider the project norm square of vector $\mathbf{h}$ onto B normalized vectors, $\mathbf{w}_j, j = 1, ..., B$, i.e., $b_j = |\mathbf{h}^T\mathbf{w}_j|^2, j = 1, 2, ..., B$, and focus again on the lth largest one among totally B projection norm square, i.e. $b_{l:B}$. Since $\mathbf{w}_j$ are not necessarily orthogonal with one another, the projection norm squares no longer constitute a set of independent random variables. To overcome such difficulty, we rewrite $b_{l:B}$ as:

$$b_{l:B} = rank_l\{|\frac{\mathbf{h}^T}{||\mathbf{h}^T||}\mathbf{w}_j|^2\} \cdot ||\mathbf{h}^T||^2 = u \cdot v. \tag{2.7}$$

It can be shown that $|\frac{\mathbf{h}^T}{||\mathbf{h}^T||}\mathbf{w}_j|^2$ follows i.i.d. beta distribution with parameters 1 and $N-1$, with PDF given by:

$$f_\beta(x) = (N-1)(1-x)^{N-2}, x \in (0, 1). \tag{2.8}$$

Now u becomes lth largest one of B i.i.d. beta random variables, whose PDF can be obtained as:

$$f_u(x) = \frac{B!(N-1)}{(B-l)!(l-1)!} \cdot \sum_{i=0}^{B-l}\binom{B-l}{i}(-1)^{B-l-i} \cdot \sum_{j=0}^{A}\binom{A}{j}(-x)^{A-j}, x \in (0, 1), \tag{2.9}$$

where $A = (N-1)(B-1-i) + N - 2$.

Noting that $v = ||\mathbf{h}||^2$ follows a modified $\chi^2_{(2N)}$ distribution, with PDF given by:

$$f_v(x) = \frac{1}{(N-1)!} x^{N-1} e^{-x}, x \geq 0, \tag{2.10}$$

the PDF of $b_{l:B}$ could be obtained as the product of two random variables [45]. After several steps of computation, we have

$$f_{b_{l:B}}(z) = \frac{B!}{(B-l)!(l-1)!(N-2)!} \cdot \sum_{i=0}^{B-l} \binom{B-l}{i} (-1)^{B-l-i} \cdot \sum_{j=0}^{A} \binom{A}{j}$$
$$z^{N-1}(-1)^{A-j} I(A-j-N_m; -z), x \geq 0, \tag{2.11}$$

where

$$I(a;b) = \int_0^1 x^a e^{b/x} dx = (-b)^a \left(-\frac{\pi \csc(\pi a) b}{\Gamma(2+a)} - \frac{b\Gamma(-a)}{1+a} + \frac{(-b)^{-a} e^b}{1+a} + \frac{\Gamma(-a,-b)b}{1+a} \right). \tag{2.12}$$

Note that this result can be broadly applied in other related analysis. In Fig. 2.2, we plot the PDF of $b_{1:B}$, and find that it matches perfectly with the simulation results.

2.3.2 Sum-rate analysis

In this part, we analyze the ergodic sum rate performance of the beamforming transmission schemes under consideration. The sum rate of the proposed dual-cell random beamforming system can be calculated as:

$$R = \int_0^\infty \log_2(1+\gamma)(f_{\gamma_1}(\gamma) + f_{\gamma_2}(\gamma)) d\gamma. \tag{2.13}$$

where $f_{\gamma_1}(\gamma)$ and $f_{\gamma_2}(\gamma)$ are the PDF of received SINR of the selected users in cell 1 and 2, respectively. We now derive the exact statistics of the selected users' SINRs.

SRB

Due to the symmetry, let's consider the received SINR of selected user by BS_1, as given in (2.2), which can be rewritten as

$$\gamma_1 = \frac{\max_i |\mathbf{h}_{1i}^T \mathbf{w}_1|^2}{|\mathbf{h}_{2i}^T \mathbf{w}_2|^2 + \rho} = \frac{a_{1:K_1}}{n_i + \rho}, \tag{2.14}$$

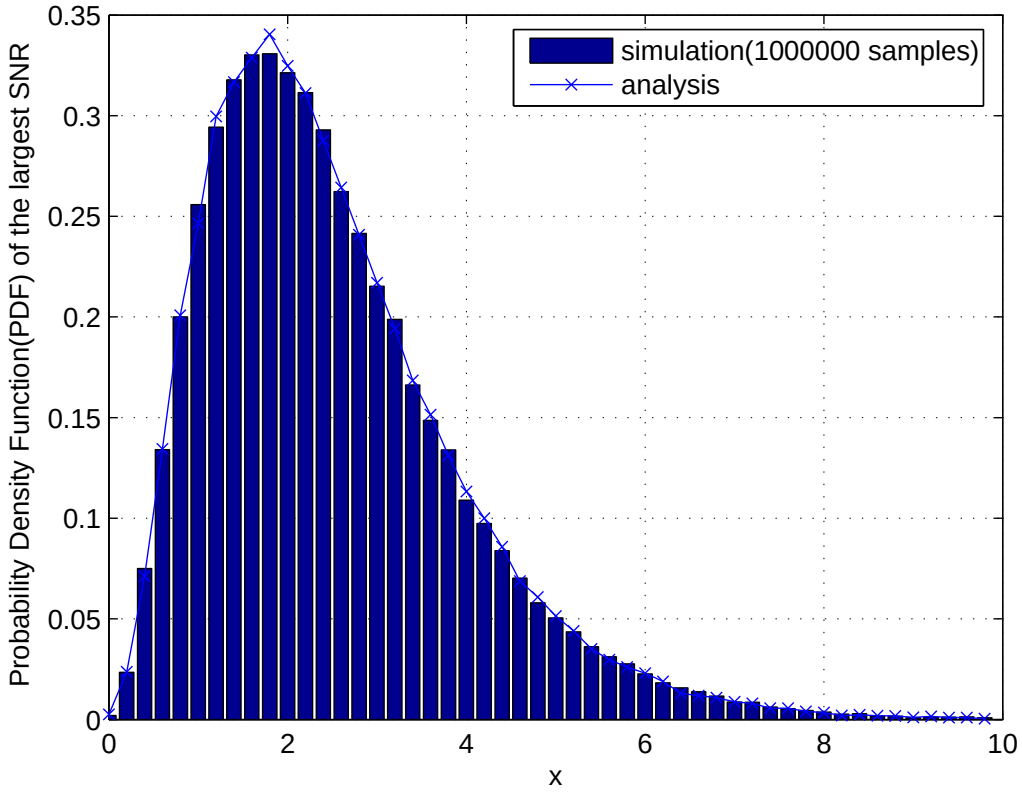

Figure 2.2: PDF of maximum projection power of a channel vector onto $B = 16$ beamforming directions $b_{1:B}$ $(N = 4)$

where n_i follows the chi-square distribution with 2 degrees of freedom, whose common PDF is represented as

$$f_{n_i}(x) = \frac{1}{\delta^2} e^{-1/\delta^2 x}. \tag{2.15}$$

And the PDF of $a_{1:K_1}$ was given in (2.6), with K changed to K_1. Noting the independence of n_i and $a_{1:K_1}$, the PDF of γ_1 can be calculated using the PDFs of n_i and $a_{1:K_1}$, as [52],

$$f_{\gamma_1}(x) = \int_0^\infty (z+\rho) f_{a_{1:K_1}}(x(z+\rho)) f_{n_i}(z) dz. \tag{2.16}$$

After carrying out the integration with proper substitutions, we have,

$$f_{\gamma_1}(x) = \frac{1}{\delta^2} \sum_{i=0}^{K_1-1} (-1)^{K_1-1-i} K_1 \times e^{-\rho(K_1-i)x} \cdot \left(\frac{\rho}{K_1 x - ix + \frac{1}{\delta^2}} + \frac{1}{(K_1 x - ix + \frac{1}{\delta^2})^2} \right). \tag{2.17}$$

IA-RB

Again due to symmetry, we consider PDF of the received SNR at the selected user by BS_2, which was given in (2.4) as the maximum of K_2 independent random variables, defined as:

$$\gamma_j' = \frac{|\mathbf{h}_{2j}^T \mathbf{w}_2|^2}{|\mathbf{h}_{1j}^T \mathbf{w}_1|^2 + \rho} = \frac{p}{q_j + \rho}. \tag{2.18}$$

Note that p term follows i.i.d. $\chi^2_{(2)}$ distribution over $\mathcal{J}$, with PDF

$$f_p(x) = e^{-x}, \tag{2.19}$$

and q_j term are i.i.d. with $\chi^2_{(2)}$ distribution over $\mathcal{J}$, but with variance δ^2, whose PDF is the same as (2.15).

Following the similar steps as for SRB, we can obtain the PDF of γ_j', $f_{\gamma_j'}(\cdot)$, as

$$f_{\gamma_j'}(x) = \frac{1}{\delta^2} e^{-\rho x} \left(\frac{\rho}{x + 1/\delta^2} + \frac{1}{(x+1/\delta^2)^2} \right). \tag{2.20}$$

It follows the CDF of γ_j', denoted by $F_{\gamma_j'}(\cdot)$, is given by

$$F_{\gamma_j'}(x) = \int_0^x f_{\gamma_j'}(y) dy = \frac{1}{\delta^2} \left(\frac{e^{-\rho x}}{-x - 1/\delta^2} + \delta^2 \right). \tag{2.21}$$

Finally, the PDF of γ_2 is obtained as,

$$f_{\gamma_2}(x) = K_2[F_{\gamma_j'}(x)]^{K_2-1} f_{\gamma_j'}(x). \tag{2.22}$$

LC-RB

Based on the notation introduced in previous subsection, the first user's SINR, can be written as,

$$\gamma_1 = \frac{\max_i |\mathbf{h}_{1i}^T \mathbf{w}_1|^2}{\min_l |\mathbf{h}_{2i^*}^T \mathbf{w}_l|^2 + \rho} = \frac{a_{1:K_1}}{b_{B:B} + \rho}. \tag{2.23}$$

The PDF of both $a_{1:K_1}$ and $b_{B:B}$ can be obtained as the special case of the general result in (2.6) and (2.11), as

$$f_{a_{1:K_1}}(x) = K_1(1 - e^{-x})^{K_1-1} e^{-x}, \tag{2.24}$$

and

$$f_{b_{B:B}}(x) = \frac{B}{(N-2)!\delta^{2N}} \cdot \sum_{j=0}^{A} \binom{A}{j} x^{N-1}(-1)^{A-j} I(A - j - N_m; -z/\delta^2), \tag{2.25}$$

respectively. Note that the element of vector $\mathbf{h}_{2i}^*$ has variance δ here.

Consequently, the PDF of γ_1 can be calculated in terms of PDFs of $a_{1:K_1}$ and $b_{B:B}$, as:

$$f_{\gamma_1}(x) = \int_0^\infty (z + \rho) f_{a_{1:K_1}}(x(z + \rho)) f_{b_{B:B}}(z) dz. \tag{2.26}$$

The statistics of the received SINR at the selected user by BS_2 is exactly the same as that of IA-RB scheme presented previously, with PDF given in (2.22).

2.3.3 Numerical examples

In this section, we present and discuss selected numerical examples to illustrate the mathematical formalism on the sum-rate analysis of the proposed coordinated beamforming schemes. Noting that all the analytical results in this chapter have been verified through Monte-Carlo simulation.

For comparison purpose, we also provide the simulation results of one of the popular conventional coordinated beamforming techniques with user selection, with CSI exchange between cells, which is called coordinated zero-forcing beamforming (CZF). Specifically, the CZF option relies on a simple multiuser scheduling method,

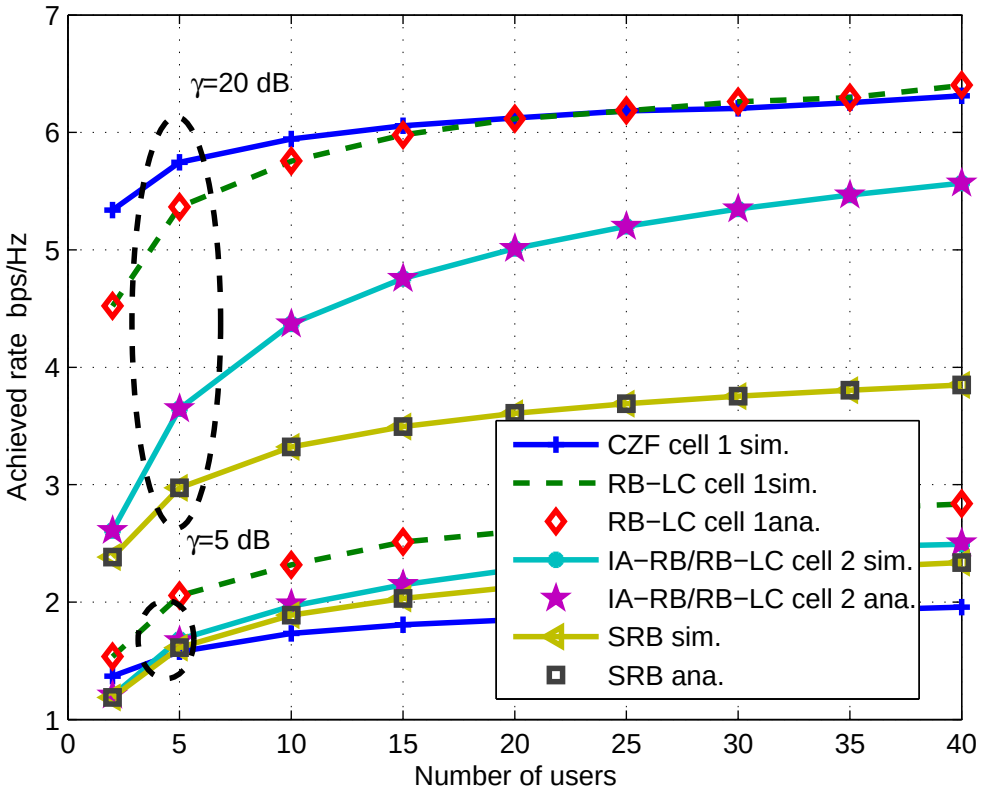

Figure 2.3: Comparison of single-cell achieved rate for different dual-cell beamforming transmission schemes (B=16, δ=0.7)

i.e. to select the user with the largest channel vector norm square. After the full CSI sharing between two cells, the new 'super BS' uses zero-forcing method to transform the interference channel into a MIMO broadcast channel [24]-[29]. Suppose that $\mathbf{h}_{1i^*}$ and $\mathbf{h}_{2j^*}$ are the two selected user's channel vectors respectively in cell 1 and 2. Then, the beamforming vector $\mathbf{w}_1$ needs to satisfy the orthogonality condition $\mathbf{h}_{1j^*}^H \mathbf{w}_1 = 0$ to cancel its interference for cell 2, .

In Fig. 2.3, we compare the single cell achieved rates for three schemes under consideration as functions of the common number of users $K = K_1 = K_2$. The radius of each cell R is 1km, the path loss exponent is 3.7, and both BSs are equipped with $N = 4$ antennas. Both analytical and simulation-based curves have been provided. It can be seen that, the SRB scheme leads to the worst performance, as its performance becomes interference limited as the number of active users increases. While both cells achieve the same rate with SRB and IA-RB, the cell 1 for LC-RB achieves the

highest rate, owing to our specific design on suppressing the inter-cell interference to the selected user from cell 2. Finally, we observe that the performance advantage of LC-RB over the other two schemes increases as the number of users increases.

2.4 Extension to Non-Identical Average Interference Power Case

As stated before, the identical average inter-cell interference power assumption only applies to the case that users are distributed along the cell-boundary. In this section, we extend to the more general scenario, where users are randomly distributed in the cell coverage.

2.4.1 SINR analysis

SRB

For the non-identical interference case, the first selected user's SINR can still be as given in (2.17). On the other hand, n_is are no longer identically distributed. The PDF of n_i becomes

$$f_{n_i}(x) = \frac{1}{\delta_i^2} e^{-1/\delta_i^2 x}. \tag{2.27}$$

After applying (2.27) into (2.17), we can obtain the PDF of γ_1 as

$$f_{\gamma_1}(x) = \frac{1}{\delta_i^2} \sum_{l=0}^{K_1-1} (-1)^{K_1-1-l} K_1 \times e^{-\rho(K_1-l)x} \cdot \left(\frac{\rho}{K_1 x - lx + \frac{1}{\delta_i^2}} + \frac{1}{(K_1 x - lx + \frac{1}{\delta_i^2})^2} \right). \tag{2.28}$$

IA-RB

For non-identical interference case, γ_j' in (2.18) are independent but not identically distributed. Specifically, the PDF of q_j becomes (2.15), but with parameter δ_j instead of common δ. Applying similar strategies as in (2.20) and (2.21), we can obtain the PDF and CDF of γ_j' for non-identical interference case as

$$f_{\gamma_j'}(x) = \frac{1}{\delta_j^2} e^{-\rho x} \left(\frac{\rho}{x + 1/\delta_j^2} + \frac{1}{(x + 1/\delta_j^2)^2} \right), \tag{2.29}$$

and

$$F_{\gamma_j'}(x) = \frac{1}{\delta_j^2}\left(\frac{e^{-\rho x}}{-x - 1/\delta_j^2} + \delta_j^2\right), \tag{2.30}$$

respectively. Therefore, we can obtain the PDF of γ_2, as,

$$f_{\gamma_2}(x) = \sum_{k=1}^{K_2} \left(\prod_{j=1, j\neq k}^{K_2} F_{\gamma_j'}(x) \right) f_{\gamma_k'}(x). \tag{2.31}$$

LC-RB

In this case, the entries of $\mathbf{h}_{2i^*}$ are i.i.d. with variance δ_{i^*}. It follows that the PDF of $b_{B:B}$ in (2.5) can be obtained as

$$f_{b_{B:B}}(x) = \frac{B}{(N-2)!\delta_i^{2N}} \cdot \sum_{j=0}^{A} \binom{A}{j} x^{N-1}(-1)^{A-j} I(A - j - N_m; -z/\delta_i^2), \tag{2.32}$$

where $I(\cdot;\cdot)$ was defined in (2.12). Applying (2.24) and (2.32) into (2.26), we can obtain the PDF of first selected user's SINR. Give the expression of f_{γ_1} after the substitution. That would make it easier to follow. Similar to identical interference case, the SINR PDF of the second selected user shares exactly the same expression as that of IA-RB scheme as given in (2.31).

2.4.2 Numerical examples

Fig. 2.4 plots the sum-rate of three dual cell transmission schemes for non-identical interference power case. It can be observed that LC-RB and IA-RB offer comparable performance gain over SRB at high SNR regime (20dB), and the three share almost the same performance at low SNR regime (5dB), owing to the tremendous noise effects. Moreover, the analysis results match perfectly with simulation results, which verifies our analytical approach. We also find the sum rate gaps between LC-RB and the other two schemes are smaller than those for the identical interference power case. It attributes to the fact that the inter-cell interference for the user can be ignorable when the distance between the selected user and its neighboring BS is large,

The observation is further confirmed in Fig. 2.5, where we examine the effect of interference strength, characterized by the distance from the selected user of cell 1 to BS_2. At high SNR regime (SNR=15 dB) and the system performance is interference-limited. The smaller the distance is, the larger the gap between LC-RB and SRB

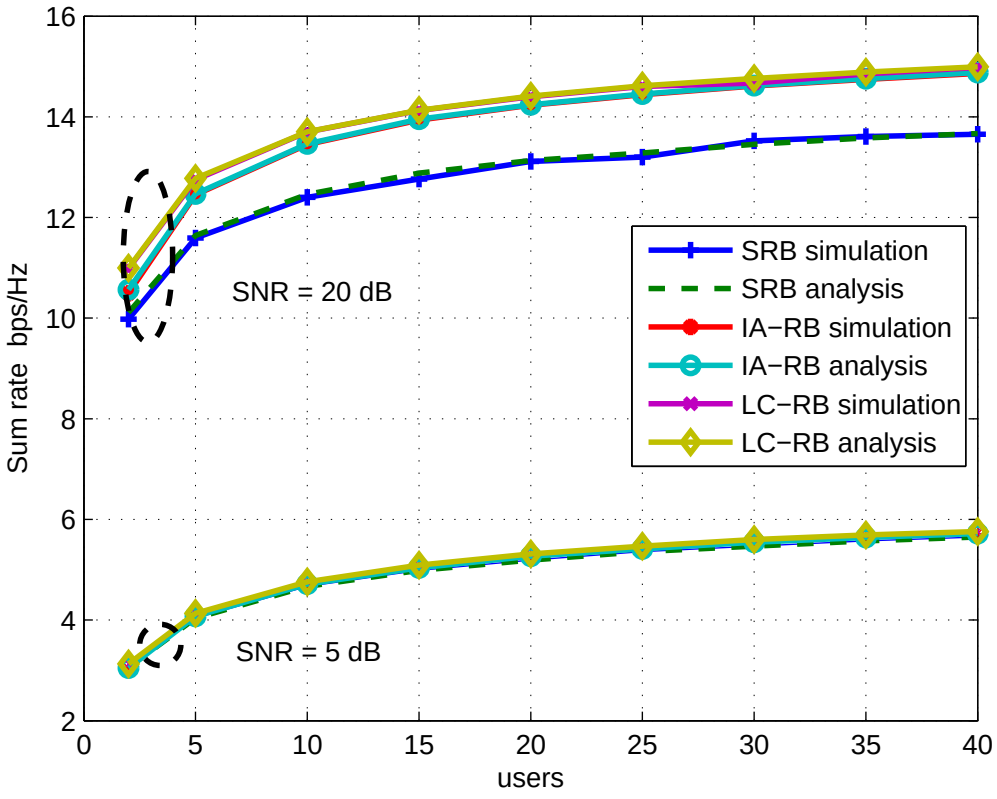

Figure 2.4: Sum-rate comparison for non-identical average interference power case

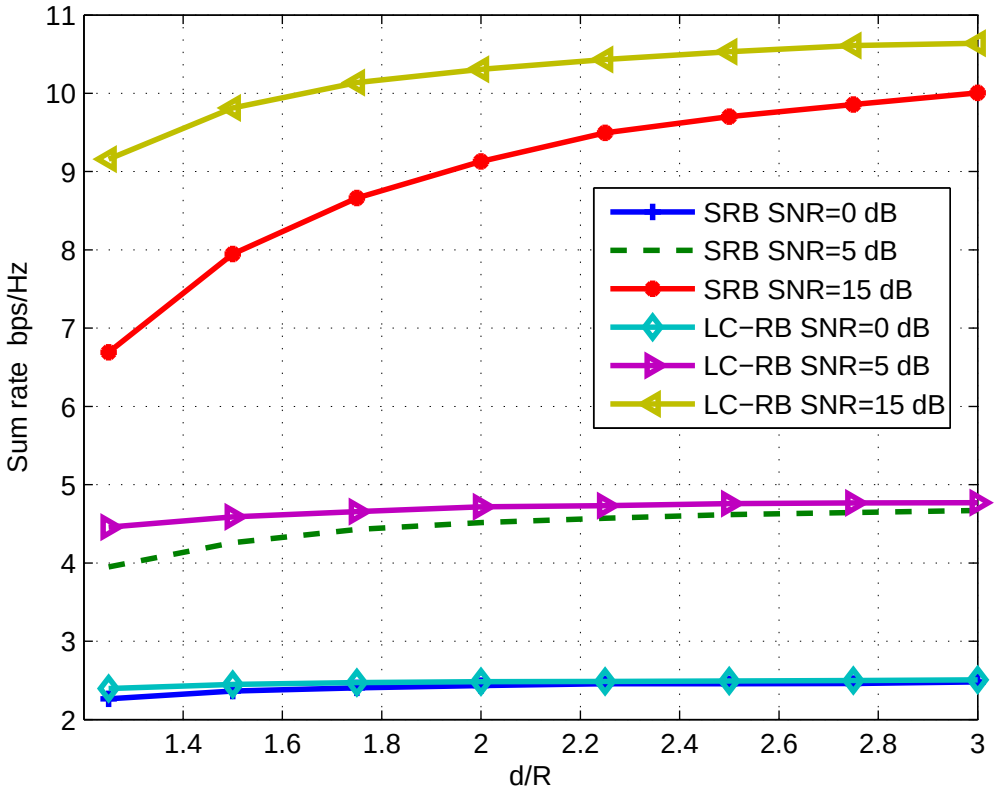

Figure 2.5: Sum-rate comparison as function of normalized distance threshold d/R (K=10)

gets, which shows the effectiveness of LC-RB on inter-cell interference control. And at medium and low SNR regime (SNR=5, 0 dB) when the overall system suffers from severe Gaussian noise, LC-RB and SRB share almost the same performance. The fact leads to the idea of adaptive implementation, to further reduce the coordination overhead while maintaining the same sum rate performance, which will be presented in the next section.

2.5 Adaptive Implementations

As stated above, there is a tradeoff between sum-rate performance versus coordination overhead between RB-LC and SRB scheme, especially when the interference is severe, i.e. the selected user is close to the neighboring BS. Specifically, if the neighboring BS is far away from the selected user, the BS may decide only to perform SRB without coordination. Noting that the decision-making process only depends on the distance information from the BS to the selected mobile user, the adaptive scheme is easy to implement.

2.5.1 Mode of operations

With adaptive implementation, the selected user of cell 1 will firstly estimate its distance to the neighboring BS based on the average interference power. If the distance is larger than a threshold, denoted by d_{TH}, and as such, the interference can be viewed as negligible, the user will suggest BS_1 to perform SRB. Otherwise, BS_1 will perform LC-RB so as to control the inter-cell interference. Note that only in the later case, the selected user of BS_1 needs to estimate the channel from the neighboring BS. Also, with the adaptive implementation, the coordination overhead is reduced and only used if necessary.

2.5.2 Coordination overload

We now quantify the average signaling overhead for coordinated beamforming with adaptive implementation. For the adaptive implementation, there are two styles of signaling message between the two BSs, depending coordination is needed or not. Specifically, if $d > d_{\mathrm{TH}}$, BS_1 sends one bit of information to BS_2 to indicate no coordination is needed, else if $d < d_{\mathrm{TH}}$, BS_1 sends the index of $\mathbf{w}_2$ in the codebook,

plus one bit of coordination indicator, which leads to $1 + \log_2 B$ bits of overhead signaling.

Based on these observations, we can easily calculate the coordination overload c for the adaptive implementation, as:

$$c = \frac{P_R}{\pi R^2}(\log_2 B + 1) + (1 - \frac{P_R}{\pi R^2}), \tag{2.33}$$

where P_R is the area in BS_1 that the coordination is needed, which can be calculated using some geometric analysis as

$$P_R = \pi R^2 \frac{\theta_1}{\pi} + \pi d_{\mathrm{TH}}^2 \frac{\theta_2}{\pi} - \frac{1}{2}(R^2 \sin(2\theta_1) + d_{\mathrm{TH}}^2 \sin(2\theta_2)), \tag{2.34}$$

and

$$\theta_1 = \arccos(\frac{5R^2 - d_{\mathrm{TH}}^2}{4R^2}), \theta_2 = \arccos(\frac{d_{\mathrm{TH}}^2 + 3R^2}{2R^2}). \tag{2.35}$$

2.5.3 Numerical examples

Fig. 2.6 presents the throughput of cell 1 and coordination overhead with the adaptive implementation, as the function of the normalized threshold d_{TH}, for various channel conditions. From Fig. 6(a), we can see that as d_{TH} increases, the throughput of cell increases as the system will invoke more coordination. Note that if $d_{\mathrm{TH}} = 3R$, the adaptive implementation is equivalent to the conventional LC-RB, and it reduces SRB when $d_{\mathrm{TH}} = R$. We also notice that performance improvement with larger threshold is more significant for high SNR range when the system is more interference limited. From Fig. 6(b), we can see that the coordination overload is also increasing as the threshold increases. Therefore, the threshold d_{TH} can be used to balance the tradeoff of throughput gain versus overhead signaling.

2.6 Conclusion

In this chapter, we studied the ergodic capacity of dual-cell MISO broadcast channels with low-complexity random beamforming. In particular, we derived the exact analytical expressions of the ergodic sum-rate for three schemes with the help of some new statistical results, and compared their performance in dual-cell environment. We showed through selected numerical examples that the LC-RB scheme achieves tremendous performance over SRB and IA-RB for any volume of active users, with

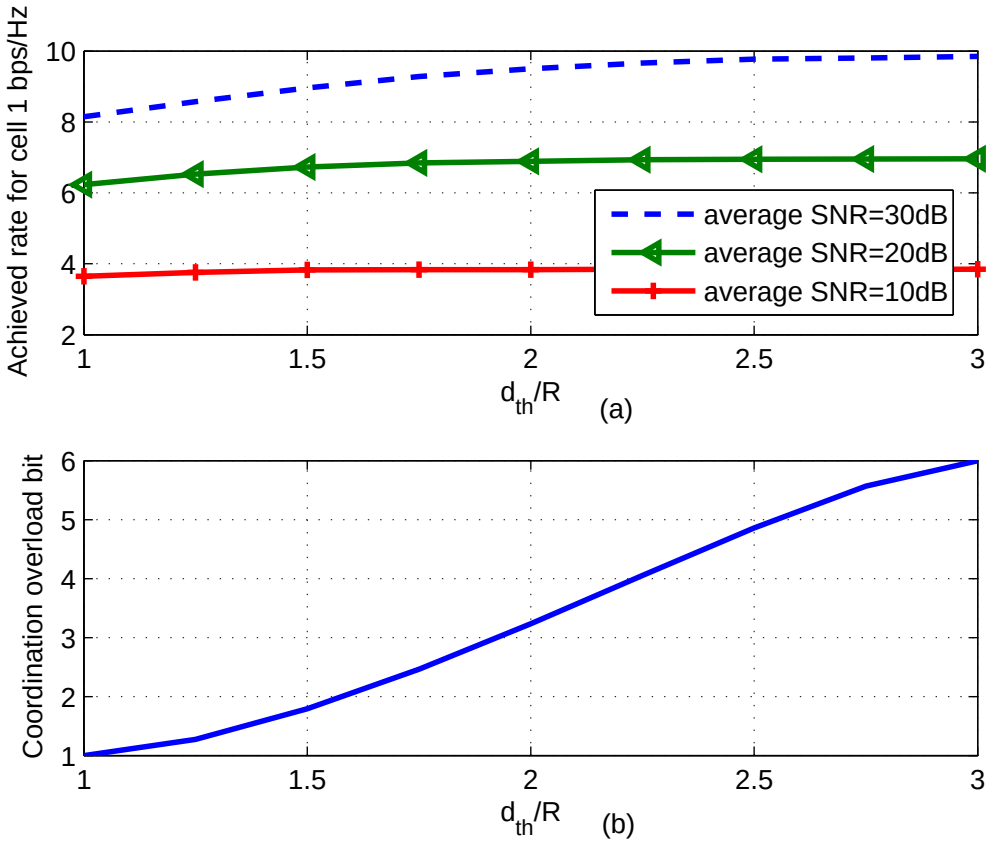

Figure 2.6: Sum-rate comparison as function of normalized distance threshold d/R (K=10)

only a beam index sharing between cells. Moreover, we have extended the scenario to the more practical case, where users are arbitrarily distributed within the overall cell coverage, and proposed an adaptive coordination scheme.

Chapter 3

Coordinated Unitary Beamforming for Dual-Cell Transmission

In this chapter, we investigate the performance of dual-cell multi-user MISO systems through statistical analysis. To limit the amount of overhead signal between BSs and minimize the additional burden to the back-haul connections, we consider the user selection scheme that exchange limited amount of control information to achieve coordinated beamforming. Instead of asymptotic analysis according to most of the literature, which assumes that the number of users is very large we address the exact sum rate analysis. We focus on coordinated beamforming strategy with random unitary codebook. Specifically, we provide an exact expression of the sum rate, based on which we can study the relation between sum rate and various system parameters including the number of transmit and receive antennas, the number of users, feedback load, and SNR. Analysis and simulation work together demonstrate that at medium and high SNR range with rich candidate users, eliminating one beam that leads to the maximum interference will always reach the best throughput performance.

The rest of the chapter is organized as follows. In Section 3.1, the system and channel models are introduced. Section 3.2 presents the proposed beam design and user selection strategies. The sum-rate analysis of the proposed system for two different user distribution scenarios is given in Section 3.3 and Section 3.4, respectively. The paper concludes in Section 3.5.

3.1 System and Channel Models

The system and channel model is similar to the ones in Chapter 2. We assume that, with proper power control mechanism, the users experience homogeneous Rayleigh fading with respect to their target BS. Thus, each component of $\mathbf{h}_{1i}$ and $\mathbf{h}_{2j}$ is modeled as independent and identically distributed (i.i.d) complex Gaussian random variables with zero mean and unit variance. When mobile users are randomly populated in their specific cell coverage area, the average received interference power is dynamic, due to the various distances from the neighboring BS to the users. Each component of the interference channel vector, $\mathbf{h}_{1j}$ and $\mathbf{h}_{2i}$ is modeled as independent complex Gaussian random variables with zero mean and variance δ_j (resp. δ_i) with respect to user j (resp. i). As will be seen in later section, we will focus mostly on the interference channel from BS_2 to the selected user in cell 1, denoted by $\mathbf{h}_{2i^*}$.

We assume that each component of $\mathbf{h}_{2i^*}$ is modeled as i.i.d. complex Gaussian random variables with zero mean and a common variance δ_{i^*}. For the special case that the mobile users are distributed along the cell boundary (depicted in Fig. 2.1(a)), and thus all the users have approximately the same distance with the neighboring BS, we can assume each component of $\mathbf{h}_{1j}$ and $\mathbf{h}_{2i}$ is modeled as i.i.d. complex Gaussian random variable with zero mean and variance δ, i.e. $\delta_i = \delta_j = \delta$ for all i and j [1]. We assume that each base station employs a codebook-based random beamforming strategy to serve one selected user in its coverage area. The codebook $\mathcal{U}$ is a N-dimension unitary matrix, i.e. $\mathcal{U}^H\mathcal{U} = \mathbf{I_N}$, randomly generated from an isotropic distribution [51]. With their wired connection to the switching center, the BSs can exchange a limited amount of control information for coordinated beamforming transmission. Specifically, the BS can communicate the utilized beamforming vectors to each other and to the users using the index of the codebook. With the proper design of the beamforming vectors and user selection, the inter-cell interference can be controlled. The specific design and selection scheme proposed in this work will be discussed in the following sections. For the multi-transmit antenna case under consideration, the received signal at the ith user in cell 1 and jth user in cell 2 can be written as:

$$\begin{aligned} y_i &= \mathbf{h}_{1i}^T\mathbf{w}_1 s_1 + \mathbf{h}_{2i}^T\mathbf{w}_2 s_2 + n_i, i \in \mathcal{I}, \\ y_j &= \mathbf{h}_{2j}^T\mathbf{w}_2 s_2 + \mathbf{h}_{1j}^T\mathbf{w}_1 s_1 + n_j, j \in \mathcal{J}. \end{aligned} \tag{3.1}$$

[1] We consider the common variance δ case for analysis consistency and tractability, which can easily be extended into the various variance case (depicted in Fig. 2.1(b)).

respectively, where $s_i (i = 1, 2)$ are data symbols to selected users and $\mathbf{w}_i (i = 1, 2)$ are the corresponding beamforming vectors, n_i and n_j are the additive Gaussian noise.

3.2 Beam Design and User Selection Strategies

In this section, we present the fundamental principles and the mode of operations of the unitary codebook-based beam design and user selection strategy, namely Multiple Interference Beam Selection (Mul-IBSS) in the dual-cell environment.

- Without loss of generality, we assume that BS_1 starts its user and beam selection for beamforming transmission first. In particular, BS triggers the communication by notifying each user in cell 1 to estimate its received signal to noise ratio (SNR) on different beamforming directions defined by its code vectors, which is proportional to $|\mathbf{h}_{1i}^T \mathbf{w}_{1k}|^2$, and then feedbacks the maximum SNR on all beams together with the index of the beam that achieves the maximum.

- BS_1 will select the user achieving the largest SNR among all users , i.e. user i^*, where $i^* = \arg\max_{i,l} |\mathbf{h}_{1i}^T \mathbf{w}_{1l}|^2, l = 1, 2, ..., N$, and use the corresponding beamforming vector as $\mathbf{w}_{1*}$. Unlike conventional random beamforming strategy, where transmission will then start without any mechanism for controlling the interference from the other base station, with the proposed coordinated transmission strategy, user i^* will estimate its MISO channel from the interfering BS, denoted by $\mathbf{h}_{2i^*}$. Based on the channel state information, user i^* will determine the beamforming vectors that can be used by the BS without introducing too much interference. For that purpose, user i^* will feedback the index of those qualified beams that will lead to the rth to Nth largest interference. BS_2 will only use those satisfying beamforming vectors for transmission.

- BS_2 will then begin its beam and user selection. Note that BS_2 will only use a subset of its available beams, as per the interference requirement of the selected user for BS_1. Specifically, every user in the coverage area of cell 2 will estimate its received signal to noise and interference ratio (SINR) on different beamforming directions defined by its code vectors, with signal power proportional to $|\mathbf{h}_{2j}^T \mathbf{w}_{2\tilde{l}}|^2$ and interference power to $|\mathbf{h}_{1j}^T \mathbf{w}_{1*}|^2$, and then feedbacks the maximum SINR on all qualified beams together with the index of the beam achieving maximum SINR. BS_2 will select the user achieving the largest SINR among all

users and use the user's best beam as $\mathbf{w}_{2*}$, i.e. user j^*, where $j^* = \arg\max_j \gamma_{2,j}$, following with

$$\gamma_{2,j} = \max_{\tilde{l}} \left(\frac{|\mathbf{h}_{2j}^T \mathbf{w}_{2\tilde{l}}|^2}{|\mathbf{h}_{1j}^T \mathbf{w}_{1*}|^2 + \rho} \right), \tag{3.2}$$

where $\tilde{l}$ is the index of the qualified beams.

Based on the above mode of operation, we can determine the SINRs of the selected users as

$$\gamma_1 = \frac{|\mathbf{h}_{1i^*}^T \mathbf{w}_{1*}|^2}{|\mathbf{h}_{2i^*}^T \mathbf{w}_{2*}|^2 + \rho} = \frac{\max_{i,l} |\mathbf{h}_{1i}^T \mathbf{w}_{1l}|^2}{|\mathbf{h}_{2i^*}^T \mathbf{w}_{2*}|^2 + \rho}, \tag{3.3}$$

and

$$\gamma_2 = \max_{j,\tilde{l}} \left(\frac{|\mathbf{h}_{2j}^T \mathbf{w}_{\tilde{l}}|^2}{|\mathbf{h}_{1j}^T \mathbf{w}_{1*}|^2 + \rho} \right), \tag{3.4}$$

where $\mathbf{w}_{2\tilde{l}}$ is selected from a subset of the original beam sets, which meet the requirement described above, and ρ is the normalized noise power.

3.3 Sum-rate Analysis for Common Variance δ

In this section, we analyze the ergodic sum rate performance of the proposed coordinated beamforming scheme for the scenario that users are located to the cell boundary as depicted in Fig. 2.1(a). In the following analysis, we firstly consider two extreme cases of Mul-IBSS, i.e. the Minimum Interference Beam Selection Strategy (Min-IBSS) when $r = N$, and the Maximum Interference Beam Elimination Strategy (Max-IBES) when $r = 2$. Based on the analysis of the two extreme cases, we address the analysis of the general Mul-IBSS.

The ergodic capacity of the dual-cell system with codebook based coordinated beamforming can be calculated as:

$$R = \int_0^\infty \log_2(1+\gamma)(f_{\gamma_1}(\gamma) + f_{\gamma_2}(\gamma))d\gamma. \tag{3.5}$$

where $f_{\gamma_1}(\gamma)$ and $f_{\gamma_2}(\gamma)$ are the PDFs of the selected users' SINR, which will be obtained for each case under consideration in the following.

We firstly derive the statistics of norm squares, $\alpha_{i,j} = |\mathbf{w}_i \mathbf{h}_j|^2$, where $\mathbf{w}_i, i = 1, ..., N$ is a set of orthogonal unit normalized vectors, and $\mathbf{h}_j, j = 1, ..., K$ follows i.i.d. complex Gaussian random variables with zero mean and variance δ. Note that $\alpha_{i,j}$ are i.i.d. chi-square random variables with two degrees of freedom [52]. Let $\alpha_{l:NK}$

be the lth largest variable among all NK ones. Thus, the probability density function (PDF) of $\alpha_{l:NK}$, $f_{\alpha_{l:NK}}(x)$can be derived as:

$$f_{\alpha_{l:NK}}(x) = \frac{(NK!)}{(NK-l)!(l-1)!\delta^2}\left(1-e^{-\frac{x}{\delta^2}}\right)^{NK-l}\cdot e^{-\frac{lx}{\delta^2}}. \tag{3.6}$$

3.3.1 Minimum interference beam selection strategy (Min-IBSS)

If $r = N$, the Mul-IBSS scheme degenerates to Min-IBSS, i.e. BS_2 can only use the beam for transmission which leads to the minimum interference to the selected user cell 1. Based on the notation introduced in the previous section, the first user's SINR for Min-IBSS, can be written as,

$$\gamma_1 = \frac{\max_{i,l}|\mathbf{h}_{1i}^T\mathbf{w}_{1l}|^2}{\min_l|\mathbf{h}_{1i^*}^T\mathbf{w}_{2l}|^2+\rho} = \frac{m}{n+\rho}. \tag{3.7}$$

The PDF of both m, denoted as $f_m(x)$ and n, as $f_n(x)$ can be obtained as the special case of the general result in (3.6), as

$$f_m(x) = K_1N(1-e^{-x})^{K_1N-1}e^{-x},\ f_n(x) = \frac{N}{\delta^2}e^{-\frac{N}{\delta^2}x}. \tag{3.8}$$

According to [52], conditioning on m, we can write the PDF of γ_1, $f_{\gamma_1}(x)$, as,

$$f_{\gamma_1}(x) = \frac{K_1N^2}{\delta^2}\int_o^\infty (z+\rho)(1-e^{-x(z+\rho)})^{K_1N-1} e^{-x(z+\rho)}e^{-\frac{N}{\delta^2}z}dz. \tag{3.9}$$

After carrying out the integration with proper substitutions, we have obtained the closed-form expression of $f_{\gamma_1}(x)$,

$$f_{\gamma_1}(x) = \frac{K_1N^2}{\delta^2}\sum_{i=0}^{K_1N-1}\binom{K_1N-1}{i}(-1)^{K_1N-1-i} e^{-\rho(K_1N-i-i)x}\left(\frac{\rho}{(K_1N-1-i)x+\frac{N}{\delta^2}}+\frac{1}{((K_1N-1-i)x+\frac{N}{\delta^2})^2}\right). \tag{3.10}$$

Alternatively, under Min-IBSS, the second user's SINR is expressed as,

$$\gamma_2 = \max_j\left(\frac{|\mathbf{h}_{2j}^T\mathbf{w}_{2*}|^2}{|\mathbf{h}_{1j}^T\mathbf{w}_{1*}|^2+\rho}\right) = \max_j\gamma_{2,j}. \tag{3.11}$$

The PDF and cumulative density function (CDF) of $\gamma_{2,j}$ can be derived that

$$\begin{aligned} f_{\gamma_{2,j}}(x) &= \tfrac{e^{-\rho x}}{\delta^2} \int_0^\infty (z+\rho) e^{-(x+\frac{1}{\delta^2}z)} dz \\ &= \tfrac{e^{-\rho x}}{\delta^2} \left(\tfrac{\rho}{(x+\frac{1}{\delta^2})^2} + \tfrac{\rho}{x+\frac{1}{\delta^2}} \right), \end{aligned} \tag{3.12}$$

and

$$F_{\gamma_{2,j}}(x) = \int_0^x f_{\gamma_k}(z) dz = \frac{1}{\delta^2} \left(\frac{e^{-\rho x}}{-x - \frac{1}{\delta^2}} + \delta^2 \right), \tag{3.13}$$

respectively. Combining $f_{\gamma_{2,j}}(x)$ and $F_{\gamma_{2,j}}(x)$ together, the PDF of the second user's SINR, $f_{\gamma_2}(x)$ can be written as,

$$f_{\gamma_2}(x) = K_2 \left(F_{\gamma_{2,j}}(x) \right)^{K_2 - 1} f_{\gamma_{2,j}}(x). \tag{3.14}$$

3.3.2 Maximum interference beam elimination strategy (Max-IBES)

In this case, BS_2 can not use the beam that leads to the maximum interference to the selected user cell 1. The first user's SINR, under Max-IBES, denoted as γ_1 is represented as:

$$\gamma_1 = \frac{|\mathbf{h}_{1i^*}^T \mathbf{w}_{1*}|^2}{|\mathbf{h}_{2i^*}^T \mathbf{w}_{2*}|^2 + \rho} = \frac{\max_{i,l} |\mathbf{h}_{1i}^T \mathbf{w}_{1l}|^2}{z_2^N + \rho} = \frac{y}{z_2^N + \rho}, \tag{3.15}$$

where z_k^N denotes one of the kth to the Nth largest modified chi-square random variable with two degrees of freedom, whose PDF can be obtained as

$$f_{z_2^N}(x) = \frac{1}{N-1} \left(\sum_{l=2}^{N} \frac{N! (1 - e^{-\frac{1}{\delta^2}x})^{N-l} e^{-\frac{lx}{\delta^2}}}{l!(N-l)!\delta^2} \right). \tag{3.16}$$

It is easy to find the PDF of y from (3.6), as:

$$f_y(x) = K_1 N (1 - e^{-x})^{K_1 N - 1} e^{-x}. \tag{3.17}$$

Conditioning on y, the PDF of γ_1 is represented as,

$$\begin{aligned} f_{\gamma_1}(x) = \tfrac{K_1 N N!}{N-1} \int_0^\infty (z+\rho)(1 - e^{-x(z+\rho)})^{K_1 N - 1} e^{-x(z+\rho)} \\ \left(\textstyle\sum_{l=2}^{N} \frac{N! (1 - e^{-\frac{1}{\delta^2}z})^{N-l} e^{-\frac{lz}{\delta^2}}}{l!(N-l)!\delta^2} \right) dz, \end{aligned} \tag{3.18}$$

Through integrations and manipulations, we obtain the following closed-form expression of $f_{\gamma_1}(x)$,

$$\begin{aligned} f_{\gamma_1}(x) = & \tfrac{1}{N-1} \textstyle\sum_{l=2}^{N} \tfrac{K_1 N N!}{(N-l)!(l-1)!\delta^2} \sum_{i=0}^{K_1 N-1} \binom{K_1 N-1}{i} \\ & (-1)^{K_1 N-i-1} e^{-\rho x (K_1 N-i-1)} \textstyle\sum_{j=0}^{B-l} \binom{B-l}{j} (-1)^{B-l-j} \\ & \left(\tfrac{\rho}{(K_1 N-1-i)x + \frac{1}{\delta^2}(B-l-j)} + \tfrac{1}{((K_1 N-1-i)x + \frac{1}{\delta^2}(B-l-j))^2} \right). \end{aligned} \tag{3.19}$$

The second user's SINR, denoted by γ_2 is represented as:

$$\gamma_2 = \frac{|\mathbf{h}_{2j^*}^T \mathbf{w}_{2*}|^2}{|\mathbf{h}_{1j} \mathbf{w}_{1*}|^2 + \rho} = \max_j \{ \frac{\max_{\tilde{l}} |\mathbf{h}_{2j}^T \mathbf{w}_{2\tilde{l}}|^2}{|\mathbf{h}_{1j}^T \mathbf{w}_{1*}|^2 + \rho} \} = \max_j \{\gamma_j\}, \tag{3.20}$$

and PDF of γ_2 is simply expressed as,

$$f_{\gamma_2}(x) = K_2 F_{\gamma_j}(x)^{K_2 - 1} f_{\gamma_j}. \tag{3.21}$$

Similar with the strategy to γ_2 in (3.12), we have obtained the CDF and PDF of γ_j, respectively, as,

$$\begin{aligned} f_{\gamma_j}(x) = & (N-1) \textstyle\sum_{i=0}^{N-2} \binom{N-2}{i} (-1)^{N-2-i} \tfrac{e^{-(N-1-i)\rho x}}{\delta^2} \\ & \left(\tfrac{1}{[(N-1-i)x + \frac{1}{\delta^2}]^2} + \tfrac{\rho}{(N-1-i)x + \frac{1}{\delta^2}} \right). \end{aligned} \tag{3.22}$$

and

$$\begin{aligned} F_{\gamma_j}(x) = & (N-1) \textstyle\sum_{i=0}^{N-2} \binom{N-2}{i} \\ & (-1)^{N-2-i} \cdot \tfrac{\rho}{(N-1-i)\delta^2} \tfrac{e^{-(N-1-i)\rho x}}{-(N-1-i)\rho x + \frac{\rho}{\delta^2}}, \end{aligned} \tag{3.23}$$

3.3.3 Multiple interference beam selection strategy (Mul-IBSS)

Recalling SINR expressions for general Mult-IBSS strategy in (3.3) and (3.4), it can be observed that the analysis method for Max-IBES can be extended to the general Mul-IBSS. Specifically, for γ_1 in (3.15), the z_2^N term in (3.15) will be replaced by z_r^N.

Thus, we have,

$$f_{z_r^N}(x) = \frac{1}{N-r+1}\left(\sum_{l=r}^{N} \frac{N!(1-e^{-\frac{1}{\delta^2}x})^{N-l}e^{-\frac{lx}{\delta^2}}}{l!(N-l)!\delta^2}\right). \tag{3.24}$$

And for γ_2 in (3.20), there will be totally $N-r+1$ candidate beams for BS_2 to use for Mul-IBSS, instead of $N-1$ for Max-IBES. Thus,

$$F_{\gamma_j}(x) = (N-r+1)\sum_{i=0}^{N-r}\binom{N-r}{i}(-1)^{N-r-i}\cdot \frac{\rho}{(N-r+1-i)\delta^2}\frac{e^{-(N-r+1-i)\rho x}}{-(N-r+1-i)\rho x+\frac{\rho}{\delta^2}}, \tag{3.25}$$

and

$$f_{\gamma_j}(x) = (N-r+1)\sum_{i=0}^{N-r}\binom{N-r}{i}(-1)^{N-r-i}\frac{e^{-(N-r+1-i)\rho x}}{\delta^2} \left(\frac{1}{[(N-r+1-i)x+\frac{1}{\delta^2}]^2}+\frac{\rho}{(N-r+1-i)x+\frac{1}{\delta^2}}\right). \tag{3.26}$$

Applying similar method, the PDF of γ_1 and γ_2 for Mul-IBSS can be expressed as:

$$f_{\gamma_1}(x) = \frac{1}{N-r+1}\sum_{l=r}^{N}\frac{K_1 N N!}{(N-l)!(l-1)!\delta^2}\sum_{i=0}^{K_1N-1}\binom{K_1N-1}{i} (-1)^{K_1N-i-1}e^{-\rho x(K_1N-i-1)}\sum_{j=0}^{B-l}\binom{B-l}{j}(-1)^{B-l-j} \left(\frac{\rho}{(K_1N-1-i)x+\frac{1}{\delta^2}(B-l-j)}+\frac{1}{((K_1N-1-i)x+\frac{1}{\delta^2}(B-l-j))^2}\right), \tag{3.27}$$

and

$$f_{\gamma_2}(x) = K_2 F_{\gamma_j}(x)^{K_2-1} f_{\gamma_j}, \tag{3.28}$$

where $F_{\gamma_j}(x)$ and $f_{\gamma_j}(x)$ are given in (3.25) and (3.26), respectively.

3.3.4 Numerical examples

In this part, we present and discuss selected numerical examples to illustrate the mathematical formalism on the sum-rate analysis of the proposed coordinated beamforming scheme. Note that all the analytical results have been verified through Monte-Carlo simulation with 3,000 random channel realizations. In Fig. 3.1, we present the ergodic sum-rate for mul-IBSS strategy, including the two extreme cases, i.e. min-ISSB ($r = N$), and max-IBES ($r = 2$), as functions of the common number of users

$K_1 = K_2$, and average channel SNR. A common $\delta = .7$ suggests that we are based on the assumption that all active users are distributed along the cell edge. It is observed that when the user number is small (less than 10), and the average channel SNR is poor (below 5 dB), the proposed system would lead to approximately the same achieved rate, regardless of the value of r, which attribute to the fact that the overall system suffers from severe noise effects, and cannot enjoy plenty of multiuser diversity gain. At medium and high SNR regime (above 5 dB), and the system is interference-limited, eliminating only one beam that leads to the maximum interference would reach the best rate performance. When the volume of users is large (more than 20), the strategy inclines to utilize more beams for transmission for cell 2, in order to fully exploit spatial multiplexing gain and multiuser diversity gain. Thus, Max-IBES outperforms other options. In summary, focusing only on cell-boundary users (depicted in Fig. 2.1(a) $\delta = .7$), shutting off only one beam for neighboring BS during coordination would lead to better performance when channel condition is good and there are enough candidate users.

3.4 Sum-Rate Analysis for Dynamic Variance

As mentioned before, the common δ assumption only applies to the case that users are distributed along the cell-boundary, as shown in Fig. 2.1(a). The scenario of Fig. 2.1(b) is also considered, in which all users are allocated within a sector of the cell. In this case, the average interference power can no longer be considered as identical, and δ_i and δ_j are dynamic, thus, the α term in (3.15) is no longer identically distributed. The PDF of it becomes

$$f_\alpha(x) = \frac{1}{\delta_i^2} e^{1/\delta_i^2 x}. \tag{3.29}$$

Applying it into (3.24), the PDF of z_r^N is updated to

$$f_{z_r^N}(x) = \frac{1}{N-r+1} \left(\sum_{l=r}^{N} \frac{N!(1-e^{-\frac{1}{\delta_i^2}x})^{N-l} e^{-\frac{lx}{\delta_i^2}}}{l!(N-l)!\delta_i^2} \right). \tag{3.30}$$

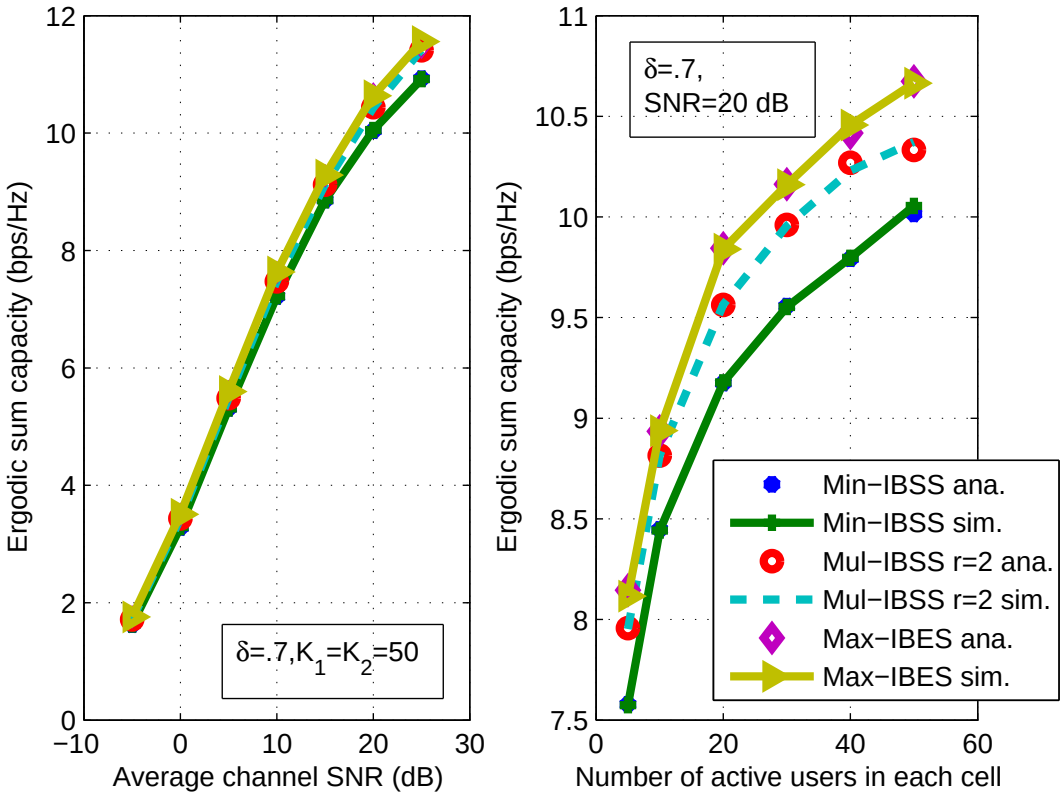

Figure 3.1: Dual-cell sum-rate comparison with respect to average channel SNR and user number ($N = 4$). A common $\delta = .7$ suggests that we assume users are allocated along the cell boundary.

Therefore, the PDF of γ_1 will be rewritten as,

$$f_{\gamma_1}(x) = \frac{1}{N-r+1} \sum_{l=r}^{N} \frac{K_1 N N!}{(N-l)!(l-1)!\delta_i^2} \sum_{i=0}^{K_1N-1} \binom{K_1N-1}{i} (-1)^{K_1N-i-1} e^{-\rho x(K_1N-i-1)} \sum_{j=0}^{B-l} \binom{B-l}{j} (-1)^{B-l-j} \left(\frac{\rho}{(K_1N-1-i)x + \frac{1}{\delta_i^2}(B-l-j)} + \frac{1}{((K_1N-1-i)x + \frac{1}{\delta_i^2}(B-l-j))^2} \right). \tag{3.31}$$

In the case of γ_2, γ_j in (3.20) are independent but not identically distributed. Specifically, the PDF of the interference term $|\mathbf{h}_{1j}^T \mathbf{w}_{1*}|^2$ in (3.20) becomes (3.29), but with parameter δ_j instead of common δ_i. Applying similar strategies as in (3.26) and (3.25), we can obtain the PDF and CDF of γ_j for non-identical interference case as

$$F_{\gamma_j}(x) = (N-r+1) \sum_{i=0}^{N-r} \binom{N-r}{i} (-1)^{N-r-i} \cdot \frac{\rho}{(N-r+1-i)\delta_j^2} \frac{e^{-(N-r+1-i)\rho x}}{-(N-r+1-i)\rho x + \frac{\rho}{\delta_j^2}}, \tag{3.32}$$

and

$$f_{\gamma_j}(x) = (N-r+1) \sum_{i=0}^{N-r} \binom{N-r}{i} (-1)^{N-r-i} \frac{e^{-(N-r+1-i)\rho x}}{\delta_j^2} \left(\frac{1}{[(N-r+1-i)x + \frac{1}{\delta_j^2}]^2} + \frac{\rho}{(N-r+1-i)x + \frac{1}{\delta_j^2}} \right). \tag{3.33}$$

Therefore, we can represent the PDF of γ_2, as

$$f_{\gamma_2}(x) = \sum_{k=1}^{K_2} \left(\prod_{j=1, j\neq k}^{K_2} F_{\gamma_j'}(x) \right) f_{\gamma_k'}(x). \tag{3.34}$$

For simulation concerns, the system parameter is set up as below: The radius of each cell R is 1km, the path loss exponent is 3.7, and both BSs are equipped with $N = 4$ antennas. Both analytical and simulation-based curves have been provided. It will be observed from Fig. 3.2 that the farther the neighboring BS is, the larger sum-rate gain. Moreover, max-IBES always provides the best sum capacity performance regardless of any channel quality or user volume.

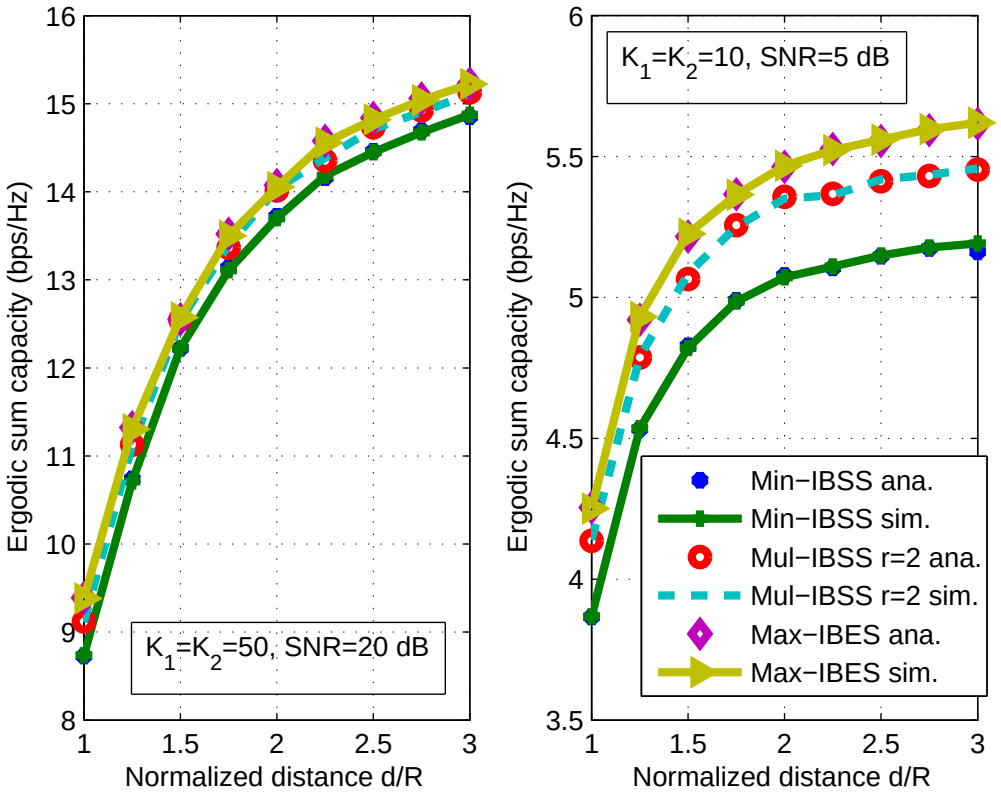

Figure 3.2: Dual-cell sum-rate comparison with respect to normalized distance to neighboring BS d/R ($N = 4$). Users are assumed to be distributed in a sector, which maximum distance to the neighboring BS is d.

3.5 Conclusion

In this chapter, we have firstly proposed a coordinated beamforming strategy based on random unitary codebook for dual-cell MISO system. Focusing on single-user scheduling in each cell, we have looked into the exact closed-form statistical analysis of selected users' SINR for the sum-rate analysis of the proposed system. Numerical results have shown that shutting off only the beam leading to the largest interference will usually lead to the best performance. On-going effort are focusing on the extension to multiuser scheduling over multiple cell scenarios.

Chapter 4

Multi-user Scheduling for Dual-cell Transmission

In this chapter, we investigate an iterative optimization algorithm which exploits the second-order cone programming (SOCP) approaches, so as to provide an optimal performance for dual-cell transmission. A more practical multi-user scheduling scheme is introduced and discussed afterwards, still based on random unitary codebook, with only certain beam index sharing between two cells. Simulation verifies the priority of the proposed scheme over traditional systems.

In order to exploit spatial multiplexing gain, multiple user scheduling case is considered afterwards. In a conventional single-cell environment, it has been fully shown that dirty paper coding (DPC) [6] can achieve optimal sum capacity for broadcast channels. However, due to its complexity in practical implementation, several near-optimal solutions are discussed, offering trade-offs between performance and complexity [46] [47]. Unfortunately, most of the work are not considering the ICI effects. The motivation of this part of the work is to provide an theoretical optimal or near-optimal performance for multi-cell transmission.

Based on the assumption that all CSI including intra-cell and inter-cell channels are available at each BS, it has been widely known that multi-cell DPC [48] offers optimal spectral efficiency, but difficult to implement. Thus, another novel block diagonalization (BD) approach is presented in [49]. Asymptotic analysis verifies the priority in performance over conventional block diagonalization. In this paper, we firstly look into the centralized optimization approach. Typically, since the sum-rate maximization problem is mostly non-convex, it is generally difficult to obtain

the globally optimum solution. Through certain approximation and relaxations, we successfully investigate an iterative optimization algorithm which exploits the second-order cone programming (SOCP) approach. From the simulation results, it can be observed that the iterative option can provide near-optimum sum capacity compared with other reference schemes, although only locally optimized. Certain other optimization work is also referred as in [50], which design objective is different from ours.

Afterwards, inspired by the successful application of Per-User Unitary Rate Control (PU^{2}RC)[13], we manage to extend it into dual-cell environment, with limited coordination between two cells. The novel strategy requires no CSI sharing between BSs, and no exact CSI feedback from users, which can be classified in the case of (2-1), and easy to implement in FDD systems. Through simulation results and comparison, the unitary codebook-based coordinated random beamforming (UCB-CRB) can provide good sum rate performance at low SNR regime, even compared with the iterative optimization results. However, the rate does not even enhance when channel SNR gets higher than 20 dB, owing to the inter-cell interference limitation.

The rest of the chapter is organized as follows. Section 4.1 presents the detailed procedure in order to investigate the SOCP optimization approach. In Section 4.2, a low-complexity coordinated beamforming transmission will be provided applied in the dual-cell scenario. Simulation results are provided in Section 4.3. The chapter concludes in Section 4.4.

4.1 Multi-user Beamforming Optimization

In this section, we are looking into a dual-cell multiuser scheduling scenario, in which both inter-cell interference and multiuser interference is considered. Typically, the system and channel models share exactly the same with the above work. The difference is, the received signal at the ith user in cell 1 and jth user in cell 2 should be replaced as:

$$\begin{aligned} y_i &= \sum_{i=1}^{N} \mathbf{h}_{1i}^T \mathbf{w}_{1i} s_{1i} + \sum_{i=1}^{N} \mathbf{h}_{2i}^T \mathbf{w}_{2i} s_{2i} + n_i, for\ i \in \mathcal{I}, \\ y_j &= \sum_{j=1}^{N} \mathbf{h}_{2j}^T \mathbf{w}_{2j} s_{2j} + \sum_{j=1}^{N} \mathbf{h}_{1j}^T \mathbf{w}_{1j} s_{1j} + n_j, for\ j \in \mathcal{J}, \end{aligned} \tag{4.1}$$

respectively, where $s_{1k}(k=i,j)$,$s_{2k}(k=i,j)$ are data symbols to selected users and $\mathbf{w}_{1i}(i=1,...,N)$, $\mathbf{w}_{2j}(j=1,...,N)$are the corresponding beamforming vectors. In this section, a joint optimization approach is under study. Since the non-convexity of the sum-rate maximization problem, there is no efficient algorithm to compute the global optimum, thus, we focus on an iterative optimization algorithm which exploits the second-order cone programming (SOCP) approaches, so as to provide significant gain, although it is locally optimal.

4.1.1 Problem formulation

In this section, we manage to formulate the overall problem to be an optimization problem. Firstly, we assume in each cell, the N scheduled users have already been selected based on certain strategies. Then, according to the previous section, we obviously can obtain the expressions of the selected users' SINRs, presented as

$$\gamma_{1i} = \frac{|\mathbf{h}_{1i}^T \mathbf{w}_{1i}|^2}{\sum_{k=1,k\neq i}^{N} |\mathbf{h}_{1i}^T \mathbf{w}_{1k}|^2 + \sum_{k=1}^{N} |\mathbf{h}_{2i}^T \mathbf{w}_{2k}|^2 + 1}; \tag{4.2}$$

$$\gamma_{2j} = \frac{|\mathbf{h}_{2j}^T \mathbf{w}_{2j}|^2}{\sum_{k=1,k\neq j}^{N} |\mathbf{h}_{2j}^T \mathbf{w}_{2k}|^2 + \sum_{k=1}^{N} |\mathbf{h}_{1j}^T \mathbf{w}_{1k}|^2 + 1}. \tag{4.3}$$

The overall problem is then formulated to be an optimization problem.

$$\begin{aligned}
&\max_{\mathbf{W}_1,\mathbf{W}_2} \quad \sum_{i=1}^{N} \log_2(1+\gamma_{1i}) + \sum_{j=1}^{N} \log_2(1+\gamma_{2j}) \\
&subject\ to: \\
&Tr\{\mathbf{W}_1\mathbf{W}_1^H\} = \sum_{i=1}^{N} ||\mathbf{w}_{1i}||^2 = P_1, \\
&\mathbf{W}_1 = [\mathbf{w}_{11}, \mathbf{w}_{12}, ..., \mathbf{w}_{1N}]; \\
&Tr\{\mathbf{W}_2\mathbf{W}_2^H\} = \sum_{j=1}^{N} ||\mathbf{w}_{2j}||^2 = P_2, \\
&\mathbf{W}_2 = [\mathbf{w}_{21}, \mathbf{w}_{22}, ..., \mathbf{w}_{2N}].
\end{aligned} \tag{4.4}$$

It can be easily verified that the optimization problem is non-convex, and thus it is difficult to obtain the globally optimum solution. In the next section, we would introduce an iterative algorithm which exploits efficient programming approaches [53] to obtain a locally optimal solution to the problem.

4.1.2 Iterative beamforming optimization

The proposed optimization algorithm is based on iterative mechanism, and after several approximations, the optimization problem in each iteration process is formulated as a convex programming problem which can be efficiently solved [53]. Without loss of generality, suppose $\mathbf{W}_1^n$ and $\mathbf{W}_2^n$ are the multiuser beamforming matrix obtained at the nth step, and

$$\mathbf{W}_1^{n+1} = \mathbf{W}_1^n + \mathbf{\Delta}_{\mathbf{W}_1}^{n+1}, \mathbf{W}_2^{n+1} = \mathbf{W}_2^n + \mathbf{\Delta}_{\mathbf{W}_2}^{n+1} \tag{4.5}$$

are the updated matrices after the $n+1$th step. Thus, the original optimization problem in the $n+1$th step is to find optimal $\mathbf{\Delta}_{\mathbf{W}_1}^{n+1}$ and $\mathbf{\Delta}_{\mathbf{W}_2}^{n+1}$ that maximizes the objective in (4.4). And the problem in the $n+1$th step can be reformulated as:

$$\begin{aligned}
&\max_{\mathbf{\Delta}_{\mathbf{W}_1}^{n+1}, \mathbf{\Delta}_{\mathbf{W}_2}^{n+1}} \quad \sum_{i=1}^{N} \left(\log_2(1+\gamma_{1i}^{n+1}) - \log_2(1+\gamma_{1i}^{n})\right) + \\
&\sum_{j=1}^{N} \left(\log_2(1+\gamma_{2j}^{n+1}) - \log_2(1+\gamma_{2j}^{n})\right), \\
&subject\ to: \quad Tr\{\mathbf{W}_1^{n+1}(\mathbf{W}_1^{n+1})^H\} = P_1, \\
&Tr\{\mathbf{W}_2^{n+1}(\mathbf{W}_2^{n+1})^H\} = P_2.
\end{aligned} \tag{4.6}$$

4.1.3 Standard-form problem setup

In order to make the optimization problem more feasible, the challenge here is to reformulate the above problem into a standard-form problem. Note that all the following operations must be based on a fundamental assumption, i.e. all the elements of both matrices, $\mathbf{\Delta}_{\mathbf{W}_1}^{n+1}$ and $\mathbf{\Delta}_{\mathbf{W}_2}^{n+1}$ are tiny. And the assumption would be added into as an additional constraints of the optimization problem. Under the assumption, several crucial steps of calculations and approximations are manipulated to transform the original problem to a standard form. Following detailed manipulations provided in Appendix A, we reformulate the problem (4.6) into a standard SOCP program:

$$\begin{aligned}
&\min_{\mathbf{x}} -\left(\sum_{i=1}^{N} \frac{\mathbf{p}_i}{(1+\gamma_{1i}^{n})} + \sum_{i=1}^{N} \frac{\mathbf{q}_j}{(1+\gamma_{2j}^{n})}\right)\mathbf{x}, \\
&subject\ to: \quad ||\mathbf{A}_i^T\mathbf{x} + \mathbf{c}_i|| \leq \mathbf{b}_i^T\mathbf{x} + d_i, i = 1, 2, 3,
\end{aligned} \tag{4.7}$$

with

$$\begin{aligned}
&\mathbf{A}_1 = \mathbf{A}^T,\ \mathbf{A}_2 = \mathbf{B}^T,\ \mathbf{A}_3 = \mathbf{I}_{4N^2\times 4N^2}.\\
&\mathbf{c}_1 = [(vec(\mathbf{W}_1)_R)^T, (vec(\mathbf{W}_1)_I)^T]^T,\\
&\mathbf{c}_2 = [(vec(\mathbf{W}_2)_R)^T, (vec(\mathbf{W}_2)_I)^T]^T, \mathbf{c}_3 = \mathbf{0}_{4N^2\times 1}.\\
&\mathbf{b}_1 = \mathbf{b}_2 = \mathbf{b}_3 = \mathbf{0}_{4N^2\times 1}.\\
&d_1 = \sqrt{P_1},\ d_2 = \sqrt{P_2},\ d_3 = \beta.
\end{aligned} \tag{4.8}$$

4.1.4 Algorithm implementation

It is obvious that the problem has already been transformed into a convex optimization problem, which implies that it can be solved efficiently with its optimal solution [53], by directly using MATLAB toolbox and other optimization software like *Sedumi*. At this point, we are now ready to present the detailed description of our proposed iterative joint beamforming optimization method in Algorithm 1.

Algorithm 1 Joint beamforming SOCP optimization

1. Select an initial point $\mathbf{x_0}$.
2. The nth iteration process: Given $\mathbf{x_n}$, using *sedumi*, find the optimal solution of $\mathbf{\Delta_x}$ by solving problem (4.7).
3. Find α^*, a value of $\alpha \in (0, 1)$ that maximizes the objective function in (4.4) with $\mathbf{x} = \mathbf{x} + \alpha^*\mathbf{\Delta_x}$, using a line search.
4. Update $\mathbf{x_{n+1}} = \mathbf{x_n} + \alpha^*\mathbf{\Delta_x}$.
5. Go back to Step 2, until $||\alpha^*\mathbf{\Delta_x}||^\mathbf{2} \leq \epsilon$.
6. Re-normalize $\mathbf{W_1}$ and $\mathbf{W_2}$, to satisfy the original power constraints.

Here, we provide some remarks on the proposed algorithms:

- Line search in Step 3 has been popular and essential to many optimization algorithms [53]. We introduce the scalar α^* through line search before updating the required beamforming vector. This scalar is utilized to guarantee the convergence of our iterative algorithm.

- Step 6 is necessary, since we have relaxed the equality constraints into inequality ones.

- Since the original problem in (4.4) is non-convex, it is generally difficult to obtain the globally optimum solution. Although this implies that the proposed

iterative optimization algorithm converges to some locally optimal solutions, numerical results still demonstrate significant performance gains.

4.2 Unitary Codebook-Based Coordinated Random Beamforming (UCB-CRB)

The previous section presents an iterative optimization approach, so as to get an near optimal sum-rate performance for the dual-cell multiuser MIMO system. However, the specific joint optimization requires exact channel vectors from all users, and the iterative scheme is not that practical and efficient especially for on-line algorithm. Thus, motivated by the Per-User Unitary Rate Control (PU^{2}RC) [54]-[55], a popular multiuser MIMO scheme applied successfully in the conventional single cell system, we would set up a modified coordinated approach, in order to extend PU^{2}RC into the multi-cell environment.

Different from the codebook setup for per-cell single user scheduling described previously in Chapter 3, we would formulate a novel codebook architecture, applied in multiuser scheduling. Specifically, codebook $\mathcal{F}$ is constituted of B code matrices, i.e. $\mathcal{F} = [\mathbf{U}_1, \mathbf{U}_2, ...\mathbf{U}_i, ...\mathbf{U}_B]$, where $\mathbf{U}_i, i = 1, 2, ..., B$ is a randomly generated N-dimensional unitary matrix. The two BSs share a common codebook for transmission, which is known both at BSs and mobile terminals. Without loss of generality, users in cell 1 calculates its own supported SINR, only considering intra-cell multiuser interference. Typically, for each user k, we have,

$$\gamma_{1k}^{i,p} = \frac{|\mathbf{h}_{1k}^T \mathbf{U}_i(:,p)|^2}{\sum_{q=1,q\neq p}^{N} |\mathbf{h}_{1k}^T \mathbf{U}_i(:,q)|^2 + \rho}, \tag{4.9}$$

where $\gamma_{1k}^{i,p}$ denotes the received SINR on the pth beam in code matrix i at user k (only considering intra-cell interference). After selecting the maximum SINR, i.e. $\gamma_{1k} = \max_{i,p} \gamma_{1k}^{i,p}$, and the indexes that lead to the maximum SINR, i.e. $[i_k^*, p_k^*] = \arg\max_{i,p} \gamma_k^{i,p}$, user k also computes the potential inter-cell interference applying beams from the matrix other than $\mathbf{U}_{i^*}$, i.e. $|\mathbf{h}_{2i}^T \mathbf{U}_j(:,t)|^2$, where $j \neq i^*$, and $t = 1, 2, ..., N$. After ranking them, user k would feedback the indexes that lead to the largest towards the rth largest inter-cell interference, denoted as I_k, combining with γ_k and $[i_k^*, p_k^*]$.

Receiving the feedback information from user k, i.e. $\{\gamma_{1k}, i_k^*, p_k^*, I_k\}$, BS_1 firstly

determines the matrix for transmission, which is denoted as $\mathbf{U}_{1^*}$, by choosing the maximum sum rate the matrix can support. Mathematically speaking,

$$1^* = \arg \max_{b=1,\ldots,B} \left(\sum_{n=1}^{N} \frac{\mathbf{h}_{1k}^T \mathbf{U}_b(:,n)}{\sum_{m=1,m\neq n}^{N} \mathbf{h}_{1k}^T \mathbf{U}_b(:,m) + \rho} \right). \tag{4.10}$$

Meanwhile, the N scheduled users in cell 1 have also been determined. According to their feedback I_k, certain beams would be notified to be shut off for cell 2's transmission. Afterwards, cell 2 begins its training in the same way as cell 1, in order to determine the transmission matrix and scheduled users. The only difference is that user k in cell 2 calculates its own supported SINR, considering both inter-cell and multiuser interference. Typically, for each user k, we have,

$$\gamma_{2k}^{i,p} = \frac{|\mathbf{h}_{1k}^T \mathbf{U}_i(:,p)|^2}{\sum_{q=1,q\neq p}^{N} |\mathbf{h}_{1k}^T \mathbf{U}_i(:,q)|^2 + \sum_{q=1}^{N} |\mathbf{h}_{1k}^T \mathbf{U}_{1^*}(:,q)|^2 + \rho}, i \neq 1^* \tag{4.11}$$

where $\gamma_{2k}^{i,p}$ denotes the received SINR on the pth beam in code matrix i at user k in cell 2. Note that $\mathbf{U}_i$ is no longer the original matrix, but containing certain shut-off beams. The algorithm is summarized in Algorithm 2, as: Here, we provide some

Algorithm 2 Unitary Matrix-Based Coordinated Random Beamforming for Dual-Cell System

0. Codebook Initialization.
1. In cell 1, for k=1,...K_1, user k calculates $\gamma_{1k}^{i,p}$ according to (4.9), and feedbacks $\gamma_{1k}, i_k^*, p_k^*, I_k$.
2. According to $\gamma_{1k}, i_k^*, p_k^*$, BS_1 selects transmission matrix $\mathbf{U}_{1^*}$, and N scheduled users.
3. I_k is forwarded to BS_2 through wired connection, in order to shut off certain beams for cell 2's transmission.
4. BS_2 broadcasts the updated codebook information to users in cell 2.
5. In cell 2, for k=1,...K_2, user k calculates $\gamma_{2k}^{i,p}$ according to (4.11), and feedbacks $\gamma_{2k}, i_k^*, p_k^*$.
6. According to $\gamma_{2k} = \max_{i,p} \gamma_{2k}^{i,p}$, i_k^*, p_k^*, BS_2 selects transmission matrix $\mathbf{U}_{2^*}$, and the scheduled users.
7. Transmission begins.

remarks on the proposed algorithms:

- The training process begins at user ends, instead of the BS, which reduces the number of handshakings between BS and mobile terminals. Feedback load

would be another concerns. Typically, for users in cell 1, it totally requires $(Q(\gamma_{1k}) + (r+1)(\log_2 N + \log_2 B))$ bits for feedback, where $Q(\cdot)$ denotes the quantized value in bits. And users in cell 2 require only $(Q(\gamma_{2k}) + (\log_2 N + \log_2 B))$ bits.

- The algorithm is mainly aimed at controlling the interference from BS_2 to cell 1. Thus, BS_1 is acted as the primary BS, while BS_2 as the slavery BS. For fairness, the two BSs should work as primary BS in turns.

- During calculation at BS, if certain beams is not reported from users, the beam would be randomly assigned to a user.

4.3 Simulation Results

This section presents simulation results of our proposed multiuser scheduling strategies, through averaging the sum rate over 3,000 random channel realizations. For UCB-CRB and selfish PU^{2}RC, we assume equal power allocation on each transmit antenna in each cell. And for other systems, we test with $P_1 = P_2$, indicating that the two cells share the same average channel power gain including the transmit power constraints and the effects of path loss. Five different strategies are provided for comparison, which are described as follows:

- Iterative joint beamforming SOCP implementation proposed in Algorithm 1. We implement the strategy with $\beta = .01$, $\epsilon = 1e-5$. And $\mathbf{W}_1 = \mathbf{W}_2 = \mathbf{I}_N$ is set to be the initial point.

- *Selfish zero-forcing (SZF) scheme*: Each cell implements zero-forcing precoding, without consideration of inter-cell interference. Therefore, $\mathbf{W}_1$ and $\mathbf{W}_2$ can be obtained through

$$\begin{aligned} \mathbf{W}_1 &= \mathbf{H}_{1i}^H(\mathbf{H}_{1i}\mathbf{H}_{1i}^H)^{-1},\ \mathbf{H}_{1i} = [\mathbf{h}_{11}, ...\mathbf{h}_{1N}], \\ \mathbf{W}_2 &= \mathbf{H}_{2j}^H(\mathbf{H}_{2j}\mathbf{H}_{2j}^H)^{-1},\ \mathbf{H}_{2j} = [\mathbf{h}_{21}, ...\mathbf{h}_{2N}]. \end{aligned} \tag{4.12}$$

- *Selfish minimum-mean-square-error (SMMSE) scheme*: Each cell implements MMSE precoding, without consideration of inter-cell interference. Therefore,

$\mathbf{W}_1$ and $\mathbf{W}_2$ can be obtained through

$$\begin{aligned}\mathbf{W}_1 &= \mathbf{H}_{1i}^H(\mathbf{H}_{1i}\mathbf{H}_{1i}^H + \mathbf{I}/P_1)^{-1},\ \mathbf{H}_{1i} = [\mathbf{h}_{11}, ...\mathbf{h}_{1N}],\\ \mathbf{W}_2 &= \mathbf{H}_{2j}^H(\mathbf{H}_{2j}\mathbf{H}_{2j}^H + \mathbf{I}/P_2)^{-1},\ \mathbf{H}_{2j} = [\mathbf{h}_{21}, ...\mathbf{h}_{2N}].\end{aligned} \tag{4.13}$$

- *Joint zero-forcing (SZF) scheme*: Two cells implement joint ZF precoding. Therefore, $\mathbf{W}_1$ and $\mathbf{W}_2$ can be obtained through

$$\begin{aligned}\mathbf{W}_1 &= \left(\mathbf{H}_1^H(\mathbf{H}_1\mathbf{H}_1^H)^{-1}\right)_{col\ 1:N},\ \mathbf{H}_1 = [\mathbf{H}_{1i}\mathbf{H}_{1j}],\\ \mathbf{W}_2 &= \left(\mathbf{H}_2^H(\mathbf{H}_2\mathbf{H}_2^H)^{-1}\right)_{col\ 1:N},\ \mathbf{H}_2 = [\mathbf{H}_{2j}\ \mathbf{H}_{2i}].\end{aligned} \tag{4.14}$$

- *Joint minimum-mean-square-error (JMMSE) scheme*: Two cells implement joint MMSE precoding. Therefore, $\mathbf{W}_1$ and $\mathbf{W}_2$ can be obtained through

$$\begin{aligned}\mathbf{W}_1 &= \left(\mathbf{H}_1^H(\mathbf{H}_1\mathbf{H}_1^H + \mathbf{I}/P_1)^{-1}\right)_{col\ 1:N},\ \mathbf{H}_1 = [\mathbf{H}_{1i}\ \mathbf{H}_{1j}],\\ \mathbf{W}_2 &= \left(\mathbf{H}_2^H(\mathbf{H}_2\mathbf{H}_2^H + \mathbf{I}/P_2)^{-1}\right)_{col\ 1:N},\ \mathbf{H}_2 = [\mathbf{H}_{2j}\ \mathbf{H}_{2i}].\end{aligned} \tag{4.15}$$

  Note that the above four approaches are all based on a simplistic user selection strategy, i.e., to select the users with the largest channel gains.

- *Selfish PU^{2}RC implementation*: Due to the symmetry, users in each cell calculate and feedback $\{\gamma_k, p_k^*, i_k^*\}$ to their own BS without considering interference from the other cell. And BS selects the transmission matrix and users according to the feedback information, respectively.

The numerical results will show the significance of utilizing properly designed beamforming schemes in order to reach a tremendous sum rate improvement in the dual-cell scenario. It will be observed that selfishly designed options, like selfish ZF, selfish MMSE, or single-cell PU^{2}RC, are not suitable any more when applying in dual-cell environment, especially when channel SNR gets higher. More specifically, we compare the ergodic dual-cell sum-rate obtained by the previously six beamforming strategies, with $N = 2$ as a function of average channel SNRs in Fig. 4.1. According to the results, it is noticed that the iterative algorithm achieves the maximum sum rate, with

the expense of comparatively high computational complexity. Thus, the achieved sum capacity can be served as an upper bound for the other proposed strategies, especially at high SNR regimes [1]. Further observation would be the UCB-CRB option, which outperforms all the others from low to medium SNRs. This result owes to the efficient user-selection strategy applied by UCB-CRB, even with no exact CSI information at BSs. On the other hand, however, the UCB-CRB performs poorly at high SNR regime, which attributes to the interference-limitation of the proposed system. Fig. 4.2 depicts the sum rate comparison under $N = 4$. Similar conclusion can be deduced from it. Comparing the two figures, the iterative algorithm and UCB-CRB can both provide more capacity gain for BSs equipped with more transmit antennas.

Focusing solely on UCB-CRB, sum capacity performance is provided for different codebook size B and value of r, as functions of number of active users. Users are assumed to be allocated in a sector, which maximum distance to the neighboring BS is $d = 1.25R$. It will be observed from Fig. 4.3 that for any channel conditions, eliminating more beams will be beneficial for enhancing the sum capacity performance. More specifically, the curves provided by $[B, r] = [4, 3]$ and $[B, r] = [8, 6]$ are similar, which suggests that $B = 4$ almost covers all the spatial freedom, so that users can fully enjoy it. Through comparing the two subfigures, we find that the proposed system does not suffer from the Gaussian noise severely, which may attributes to the heavy interference limitation.

4.4 Conclusion

In this chapter, we have investigated an iterative optimization algorithm which exploits the second-order cone programming (SOCP) approaches, so as to provide an optimal performance for dual-cell transmission. A more practical multi-user scheduling scheme has been introduced and discussed later, still based on random unitary codebook, with only certain beam index sharing between two cells. Simulation verifies the priority of the proposed scheme over traditional systems.

[1] The upper bound only applies to those schemes that are based on the simplistic user-selection strategy, but not others, like the proposed UCB-CRB

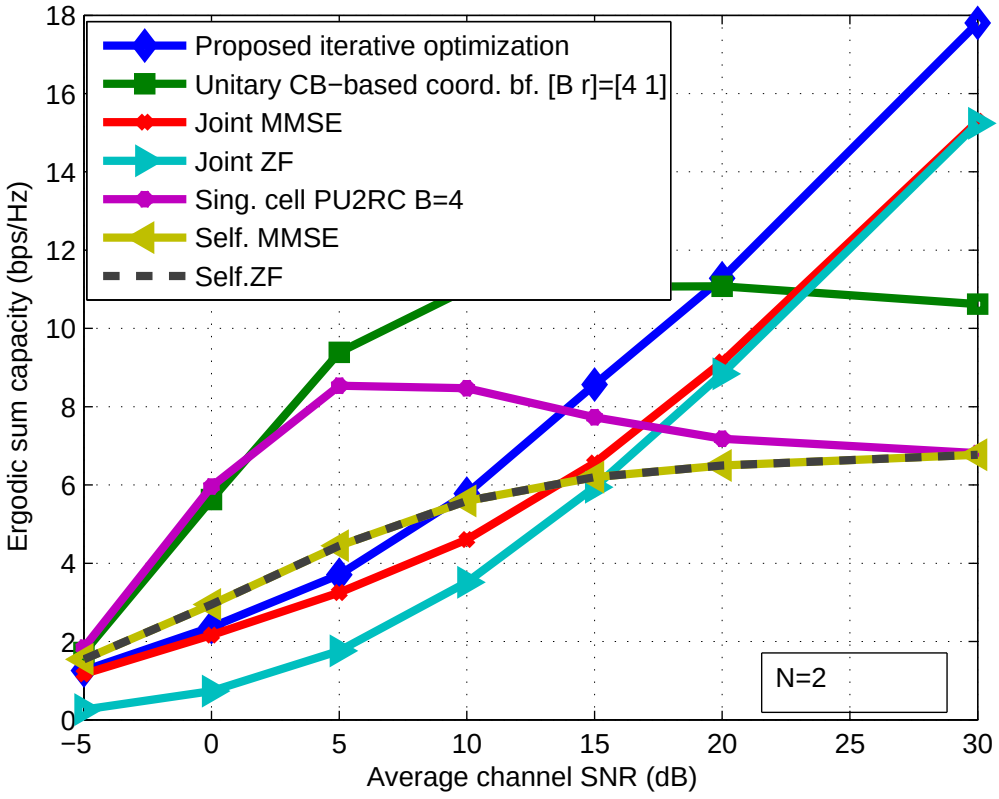

Figure 4.1: Dual-cell sum-rate comparison ($N = 2, K_1 = K_2 = 10$, and $\delta = .7$)

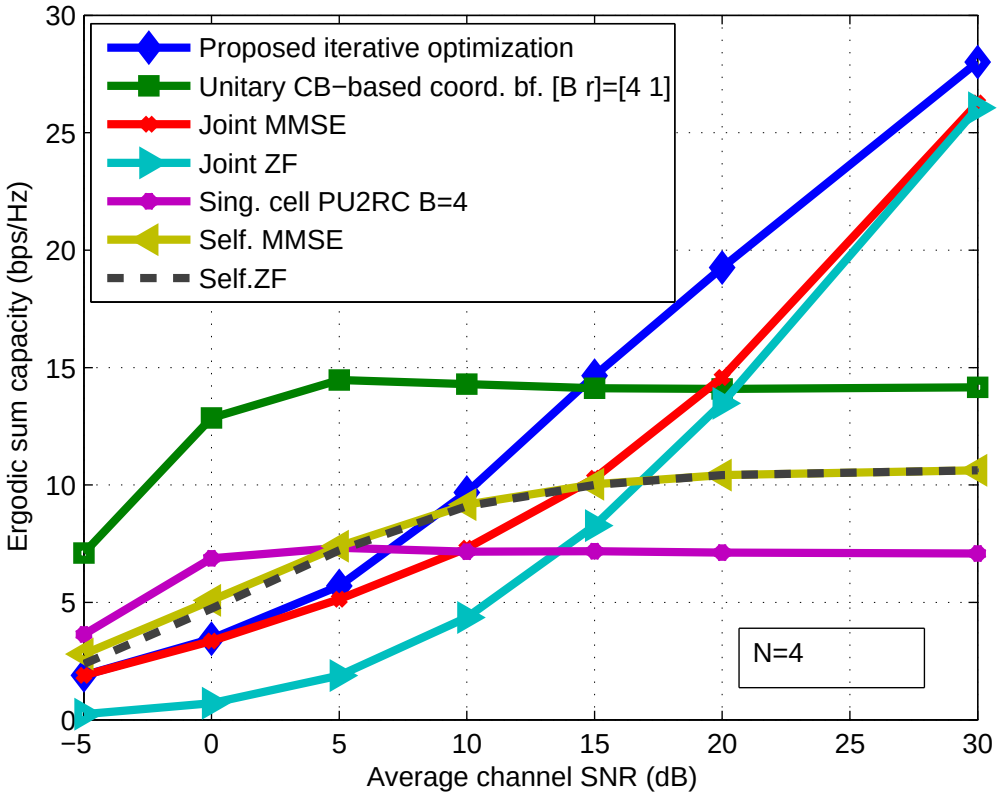

Figure 4.2: Dual-cell sum-rate comparison ($N = 4, K_1 = K_2 = 10$, and $\delta = .7$)

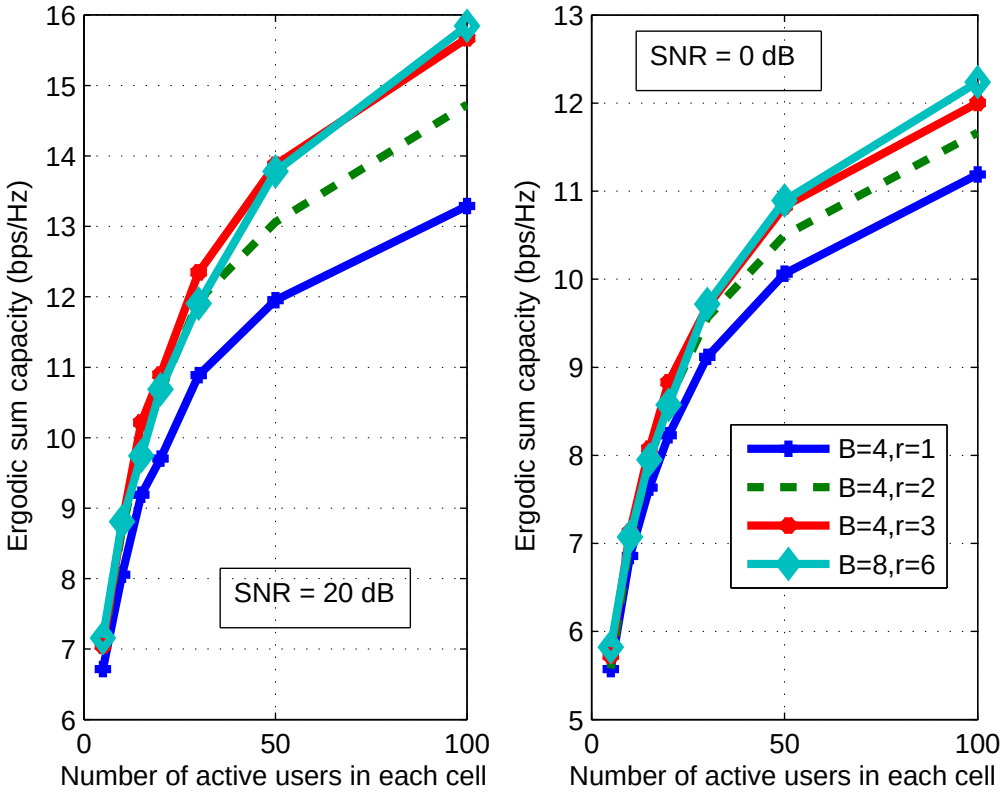

Figure 4.3: Dual-cell sum-rate comparison for different codebook size B and r ($N = 4$ and $d/R = 1.25$)

Chapter 5

Coordinated Beamforming in Two-Tier Femtocell Networks

In order to satisfy the unrelenting demand for higher data rates in wireless networks and to compete with the Wi-Fi networks, especially for home and office use, the idea of femtocell [37], has drawn tremendous research, industrial and business attention recently. A femtocell access point (FAP) is a low-power, low-cost base station that provides high data rate coverage to an indoor environment. FAP is connected to the serving base station (BS) of the cell. The key difference with Wi-Fi is that it will operate in the same licensed spectrum as the cellular network [38]. Thus, the performance of such networks would be limited by cross-tier interference [39], especially when the number of FAPs increases [14]. Therefore, interference management has become a crucial problem in the design and implementation of such two-tier systems.

Previous work has exploited the cross-tier interference control method by using time hopping with antenna sectoring [40] and transmit power control [41] for a two-tier CDMA network. In [42], two interference mitigation strategies in which femtocell users adjust the maximum transmit power for uplink channels have been proposed. For multi-antenna downlink channels, [43] has developed a beam subset selection strategy, in order to maximize the system throughput.

In this chapter, we consider the interference control with beamforming coordination in the two-tier femtocell system. To limit the amount overhead signal between BS and FAP, and minimize the additional burden to the residential DSL or broadband cable connections, we consider two schemes that exchange a small amount of control information to achieve coordinated beamforming. Specifically, we look into

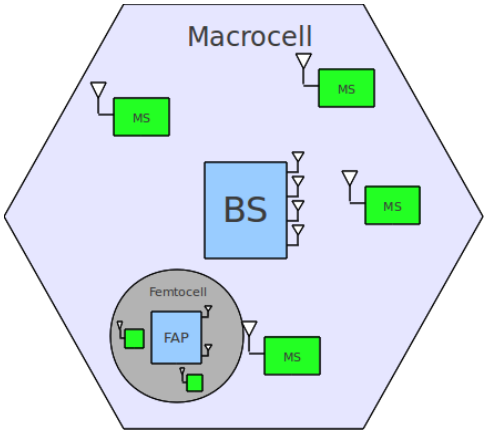

Figure 5.1: Two-tier system model

the coordinated transmission schemes for multiuser MISO systems, where only the selected beam index information are shared among the BS and FAP.

We evaluate the performance of the resulting system in terms of system throughput through accurate mathematical analysis and compare them with other design options. In particular, the exact statistics of users' SINRs are derived and applied to system throughput evaluation. Selected numerical examples show that our proposed schemes can offer significant throughput gain over other design options with a small system overhead. For analytical tractability, we only consider single user scheduling in each cell.

The rest of the chapter is organized as follows. In Section 5.1, the system and channel models are introduced. Section 5.2 presents the proposed beam design and user selection strategies for two schemes. The throughput analysis of the proposed systems is given in Section 5.3 In Section 5.4, selected numerical examples are provided and discussed. The chapter concludes in Section 5.5.

5.1 System and Channel Models

The system under consideration as shown in Fig. 5.1 consists of one BS and one FAP, utilizing the same radio spectrum to serve their selected users. [1] The BS is equipped with N_m antennas, and the FAP with N_f antennas, which facilitate beamforming

[1] In the practical system, usually one macrocell is equipped with several indoor femtocells. However, the macrocell user, for most of the cases is only effected by its nearest femtocell during transmission, due to the low transmit power of FAP. Thus, here we consider the one macrocell one femtocell case, which is fairly representative.

transmission. Each user has only a single receive antenna due to its size or complexity constraint. The user set in the macrocell is denoted by $\mathcal{I} = \{1, 2, \ldots, i, \ldots, K_1\}$, and that in femtocell by $\mathcal{J} = \{1, 2, \ldots, j, \ldots, K_2\}$. The channel vectors are defined as following,

- $\mathbf{h}_{1i}$ is the $N_m \times 1$ channel vector from the BS to the ith user in macrocell, i.e. $i \in \mathcal{I}$.
- $\mathbf{h}_{2i}$ is the $N_f \times 1$ channel vector from the FAP to the ith user in macrocell, i.e. $i \in \mathcal{I}$.
- $\mathbf{h}_{1j}$ is the $N_m \times 1$ channel vector from the BS to the jth user in femtocell, i.e. $j \in \mathcal{J}$.
- $\mathbf{h}_{2j}$ is the $N_f \times 1$ channel vector from the FAP to the jth user in femtocell, i.e. $j \in \mathcal{J}$.

We assume that, with proper power control mechanism based on average channel gain, the users experience flat homogeneous Rayleigh fading with respect to their respective serving base stations. Thus, each component of $\mathbf{h}_{1i}$ and $\mathbf{h}_{2j}$ is modeled as independent and identically distributed (i.i.d) complex Gaussian random variables with zero mean and unit variance. On the other hand, the average channel gains of the interference channels $\mathbf{h}_{1j}$ and $\mathbf{h}_{2i}$ vary with transmit power and path distance. Since femtocell users are usually closely-located around the FAP, we assume that the components of $\mathbf{h}_{1j}$ for all js is modeled as independent and identically distributed (i.i.d.) complex Gaussian random variables with zero mean and a common variance δ_1. As will be seen in later section, we will focus only on the interference channel from the FAP to the selected user in the macrocell, denoted by $\mathbf{h}_{2i^*}$. We assume that each component of $\mathbf{h}_{2i^*}$ is modeled as i.i.d. complex Gaussian random variables with zero mean and a common variance δ_2. In this scenario, δ_1 and δ_2 characterize the average received signal power from the interference source, which depends on transmit power, shadowing and path loss.

With the wired connection between the BS and the FAP, they can exchange a limited amount of control information for coordinated beamforming transmission. In particular, both the BS and the FAP employ a codebook-based random beamforming strategy to serve one selected user in their respective coverage area. We assume that the macrocell codebook has B_m unit norm column vectors of length N_m, denoted as

$\mathbf{w}_{1k}, k = 1, ..., B_m$, and the femtocell codebook contains B_f unit norm column vectors of length N_f, denoted as $\mathbf{w}_{2l}, l = 1, ..., B_f$, all generated randomly from an isotropic distribution [51]. The BS (or the FAP) will communicate the utilized beamforming vectors to each other and to the users using the index of the codebook. With the proper design of the beamforming vectors and proper user selection, the cross-tier interference can be controlled. The specific design and selection scheme proposed in this work will be discussed in the following secions. For the multi-transmit antenna case under consideration, the received signal at the ith user in macrocell and jth user in femtocell can be written as:

$$\begin{aligned} y_i &= \mathbf{h}_{1i}^T \mathbf{w}_{1*} s_1 + \mathbf{h}_{2i}^T \mathbf{w}_{2*} s_2 + n_i, i \in \mathcal{I}, \\ y_j &= \mathbf{h}_{2j}^T \mathbf{w}_{2*} s_2 + \mathbf{h}_{1j}^T \mathbf{w}_{1*} s_1 + n_j, j \in \mathcal{J}. \end{aligned} \tag{5.1}$$

respectively, where $s_i (i = 1, 2)$ are data symbols to selected users and $\mathbf{w}_{i*} (i = 1, 2)$ are the selected beamforming vectors.

5.2 Beam Design and User Selection Strategies

In this section, we present the proposed low-complexity coordinated beamforming strategies, namely angle-interference-control random beamforming (AIC-RB) and power-interference-control random beamforming (PIC-RB).

We assume that macrocell BS starts its user and beam selection for beamforming transmission first. In particular, BS triggers the communication by notifying each user in the coverage area of macrocell to estimate its received signal to noise ratio (SNR), which will be proportional to the projection power of users' channel vectors onto the different beamforming directions defined by its code vectors, i.e. $|\mathbf{h}_{1i}^T \mathbf{w}_{1k}|^2$, and then feedbacks the maximum SNR on all beams together with the index of the beam that achieves the maximum.

BS will select the user achieving the largest SNR among all users, i.e. user i^*, where $i^* = \arg\max_{i,k} |\mathbf{h}_{1i}^T \mathbf{w}_{1k}|^2$, and use the corresponding beamforming vector as $\mathbf{w}_{1*}$. Unlike conventional random beamforming strategy, where transmission will then start without any mechanism for controlling the interference from the FAP, with the proposed coordinated transmission strategy, user i^* will estimate its MISO channel from the interfering FAP, denoted by $\mathbf{h}_{2i^*}$. Based on the channel state information, user i^* will determine the beamforming vectors that can be used by the FAP without

introducing too much interference. For that purpose, we reach the following two options.

i) *Angle interference control random beamforming (AIC-RB)*: With AIC-RB, user i^* will feed back the index of the beam that will lead to the smallest interference, which acts as the center reference. The FAP will only use those beamforming vectors that form an angle smaller than the threshold with the reference beam. Mathematically speaking, the beamforming vector $\mathbf{w}_{2*}$ should satisfy

$$\mathbf{w}_{2*} \in \{\mathbf{w}_{2l} | \langle \mathbf{w}_{2l}, \mathbf{w}_R \rangle \geq \cos\theta_{\mathrm{T}}\}, \tag{5.2}$$

where θ_{T} is a threshold angle, and $\mathbf{w}_R$ satisfies,

$$\mathbf{w}_R = \arg\min_l |\mathbf{h}_{2i^*}^T \mathbf{w}_{2l}|^2. \tag{5.3}$$

ii) *Power interference control random beamforming (PIC-RB)*: With PIC-RB, user i^* will suggest that the FAP use those vectors whose resulting intercell interference power is below a threshold value. Mathematically speaking, the beamforming vector $\mathbf{w}_{2*}$ should satisfy

$$\mathbf{w}_{2*} \in \{\mathbf{w}_{2l} | \frac{|\mathbf{h}_{2i^*}^T \mathbf{w}_{2l}|^2}{\rho} \leq \alpha_{\mathrm{T}}\}, \tag{5.4}$$

where α_{T} denotes the threshold value for interference power, and ρ is the normalized noise power. Note that user i^* needs to feed back the indeces of those qualified beamforming vectors.

FAP will then begin its beam and user selection based on those information. Note that FAP will only use a subset of its beams. Specifically, every user in the coverage area of femtocell will estimate its received signal to noise and interference ratio (SINR), with signal power proportional to $|\mathbf{h}_{2j}^T \mathbf{w}_{2l}|^2$ and interference power to $|\mathbf{h}_{1j}^T \mathbf{w}_{1*}|^2$, and then feedback the maximum SINR on all beams together with the index of the beam achieving maximum SINR. FAP will select the user achieving the largest SINR among all users and use the user's best beam as $\mathbf{w}_{2*}$, i.e. user j^*, where $j^* = \arg\max_j \gamma_{2,j}$, following with

$$\gamma_{2,j} = \max_l \left(\frac{|\mathbf{h}_{2j}^T \mathbf{w}_{2l}|^2}{|\mathbf{h}_{1j}^T \mathbf{w}_{1*}|^2 + \rho} \right). \tag{5.5}$$

In summary, with the proposed scheme, the macrocell controls the interference

from the femtocell through beam subset selection, whereas the femtocell controls the interference from the macrocell by user/beam selection based on SINR.

5.3 Throughput Analysis

In this section, we analytically quantify the achieved throughput performance of the proposed scheme. In the following, we derive the statistics of the received SINR of scheduled users in the macrocell and femtocell separately.

5.3.1 Macrocell user's SINR analysis

The macrocell user's SINR, denoted as γ_m, can be written as,

$$\gamma_m = \frac{\max_{i,k} |\mathbf{h}_{1i}^T \mathbf{w}_{1k}|^2}{|\mathbf{h}_{2i^*} \mathbf{w}_{2l}|^2 + \rho} = \frac{p}{q + \rho}. \tag{5.6}$$

Noting that p is the largest projection power of all K_1 users' channel vectors onto B_m beamforming directions, its PDF can be written as,

$$f_p(x) = K_1 [F_b(x)]^{K_1 - 1} f_b(x), \tag{5.7}$$

where $f_b(x)$ is the PDF of the term $\max_k |\mathbf{h}_{1i^*}^T \mathbf{w}_{1k}|^2$, denoted as b, and $F_b(x)$ is the CDF of b. Since each $\mathbf{w}_{1k}$ has been normalized, and is not orthogonal with each other, the projections on a certain channel vector no longer constitute a set of uncorrelated variables, which is difficult to handle. Thus, we consider rewriting b as:

$$b = \max_k \{ | \frac{\mathbf{h}_{1i^*}^T}{||\mathbf{h}_{1i^*}^T||} \mathbf{w}_{1k}|^2 \} \cdot ||\mathbf{h}_{1i^*}^T||^2 = u \cdot v \tag{5.8}$$

in order to eliminate the correlations among each projection value and generate a set of independent random variables, i.e. $| \frac{\mathbf{h}_{1i^*}^T}{||\mathbf{h}_{1i^*}^T||} \mathbf{w}_{1k}|^2 = \beta$. Afterwards, it is easy to find that it experiences beta distribution with 1 and $N_m - 1$, whose PDF is expressed as:

$$f_\beta(x) = (N_m - 1)(1 - x)^{N_m - 2}, x \in (0, 1). \tag{5.9}$$

and u is the maximum value of them, shown as:

$$f_u(x) = B_m(N_m-1)\cdot\sum_{i=0}^{B_m-1}\binom{B_m-1}{i}(-1)^{B_m-1-i}\cdot\sum_{j=0}^{A}\binom{A}{j}(-x)^{A-j}, x\in(0,1),$$

where $A=(N_m-1)(B_m-1-i)+N_m-2$.

Noting that $v=||\mathbf{h}_{1i^*}||^2$ follows a modified $\chi^2_{(2N_m)}$ distribution, with PDF given by:

$$f_v(x)=\frac{1}{(N_m-1)!}x^{N_m-1}e^{-x}, \tag{5.10}$$

the PDF of the z could be obtained as the product of two random variables [45], and after several steps of computation, we have,

$$f_b(z)=\frac{B_m}{(N_m-2)!}\cdot\sum_{i=0}^{B_m-1}\binom{B_m-1}{i}(-1)^{B_m-1-i}\cdot\sum_{j=0}^{A}\binom{A}{j}z^{N_m-1}(-1)^{A-j}I(A-j-N_m;-z), \tag{5.11}$$

where $A=(N_m-1)(B_m-1-i)+N_m-2$, and

$$I(a;b)=\int_0^1 x^a e^{b/x}dx=(-b)^a\left(-\frac{\pi\csc(\pi a)b}{\Gamma(2+a)}-\frac{b\Gamma(-a)}{1+a}+\frac{(-b)^{-a}e^b}{1+a}+\frac{\Gamma(-a,-b)b}{1+a}\right). \tag{5.12}$$

Now let's consider the q term in (5.6) for both options separately.

AIC-RB

Given that there are totally B_s codewords,whose directions satisfy the angle range requirement and can be used by FAP, the term q would be one of the (B_f-B_s+1)th to the B_fth largest projection powers $|\mathbf{h}_{2i}\mathbf{w}_{2l}|^2$ random variable among the total B_f ones. The conditional PDF of q given B_s is given by,

$$f_q(x|B_s)=\frac{1}{B_s}\left(\sum_{l=B_f-B_s+1}^{B_f}f(l,z)\right), \tag{5.13}$$

where $f(l,z)$ denotes the PDF of the lth largest projection power, which can be shown to be given as,

$$f(l,z) = \frac{B_f!}{(B_f-l)!(l-1)!(N_f-2)!\delta_2^{2N_f}} \cdot \sum_{i=0}^{B_f-l} \binom{B_f-l}{i}(-1)^{B_f-l-i} \sum_{j=0}^{A} \binom{A}{j} z^{N_f-1}(-1)^{A-j} I(A-j-N_f; -z/\delta_2^2). \tag{5.14}$$

After removing the conditioning, we have

$$f_q(x) = \sum_{n=1}^{B_f} f_q(x|B_s) \cdot \Pr(B_s = n), \tag{5.15}$$

where $\Pr(B_s = n)$ stands for the probability that n codewords satisfy the angle range requirement. Note that code vectors are randomly generated. Therefore, if θ stands for the angle between the two vectors, it can be shown that $|\cos^2\theta|$ is beta distributed. It follows that the probability that the angle between two vectors is no smaller than a threshold $\lambda = \arccos\theta_{\mathrm{T}}$ is given by $\Pr[|\cos^2\theta| \geq \lambda] = (1-\lambda)^{N_f-1}$. It follows that

$$\Pr(B_s = n) = \binom{B_f}{n}(1-\lambda)^{(N_f-1)n} \cdot \left(1-(1-\lambda)^{N_f-1}\right)^{B_f-n}. \tag{5.16}$$

PIC-RB

Based on the mode of operations, the interference power would follow a truncated distribution with PDF

$$f_q(x) = \frac{f_\alpha(x)}{\int_{-\infty}^{\alpha_{\mathrm{T}}\cdot\rho} f_\alpha(x)dx}, \tag{5.17}$$

where $f_\alpha(x)$ denotes the PDF of the projection power $|\mathbf{h}_{2i^*}^T \mathbf{w}_{2l}|^2$. Therefore, the PDF of q specializes to

$$f_q(x) = \frac{e^{-\frac{1}{\delta_2^2}x}}{\delta_2^2(1-e^{-\frac{1}{\delta_2^2}\alpha_{\mathrm{T}}})}. \tag{5.18}$$

Consequently, the PDF of γ_m can be calculated in terms of PDFs of p and q, denoted by $f_p(x)$ and $f_q(x)$ respectively, as [52]:

$$f_{\gamma_m}(x) = \int_0^\infty (z+\rho) f_p(x(z+\rho)) f_q(z) dz. \tag{5.19}$$

With the PDF, we can readily evaluate the throughput of the scheduled user in

macrocell, as

$$R = \int_0^\infty \log_2(1+\gamma) f_{\gamma_m}(\gamma) d\gamma. \tag{5.20}$$

5.3.2 Femtocell user's SINR analysis

Based on the mode of operation of the proposed schemes, the femtocell user's SINR, denoted by γ_f can be written as:

$$\gamma_f = \max_j \{ \frac{\max_{k=1,\ldots,B_s} |\mathbf{h}_{2j}^T \mathbf{w}_{2k}|^2}{|\mathbf{h}_{1j^*}^T \mathbf{w}_{1*}|^2 + \rho} \}. \tag{5.21}$$

Therefore, noting the independence between user channels, the PDF of γ_f is simply expressed as,

$$f_{\gamma_f}(x) = K_2 F_{\gamma_j}(x)^{K_2 - 1} f_{\gamma_j}(x), \tag{5.22}$$

where

$$\gamma_j = \frac{\max_{k=1,\ldots,B_s} |\mathbf{h}_{2j}^T \mathbf{w}_{2k}|^2}{|\mathbf{h}_{1j^*}^T \mathbf{w}_{1*}|^2 + \rho} = \frac{m}{r+\rho}. \tag{5.23}$$

Similar to the strategy to γ_m in (5.19), we can obtain the CDF and PDF of γ_j, in terms of PDF of m and r, respectively, as,

$$F_{\gamma_j}(x) = \int_0^\infty \int_0^{x(z+\rho)} f_{m,r}(y,z) dy dz. \tag{5.24}$$

and

$$f_{\gamma_j}(x) = \int_0^\infty (z+\rho) f_m(x(z+\rho)) f_r(z) dz. \tag{5.25}$$

It can be shown that the PDFs of m and r are given by

$$f_m(x) = \sum_{n=1}^{B_f} f_b(x;n) \cdot \Pr(B_s = n), \tag{5.26}$$

and

$$f_n(x) = \frac{1}{\delta_1^2} e^{-x/\delta_1^2}, \tag{5.27}$$

respectively, where $f_b(x;n)$ is the same as $f_b(x)$ in (8), with B_m replaced by n, $\Pr(B_s = n)$ was given in eq. (5.16) for AIC-RB, and in

$$\Pr(B_s = n) = \binom{B_f}{n} \left(\int_{-\infty}^{\alpha_{\mathrm{T}}} f_X(x)dx \right)^n \left(1 - \int_{-\infty}^{\alpha_{\mathrm{T}}} f_X(x)dx \right)^{B_f - n} \tag{5.28}$$

for PIC-RB. Finally, after successive substitutions, the PDF of γ_f can be obtained, but omitted for conciseness.

5.4 Numerical Examples

In this section, we present selected numerical examples in order to illustrate the mathematical formalism on the throughput analysis of the proposed coordinated beamforming schemes in the two-tier network. Noting that all the analytical results in this chapter have been verified through Monte-Carlo simulation. We assume in the numerical examples that BS is equipped with $N_m = 4$ antennas, while FAP with $N_f = 2$. There are totally $K_1 = 40$ active users in the macrocell, and $K_2 = 4$ users in the femtocell.

Fig. 5.2 shows the achieved rate of the macrocell user in the proposed system with PIC-RB as the function of δ_2 in comparison with the no coordination case, i.e. the BS and the FAP select the beam and user by choosing the maximum SNR on all beams from all its users in the coverage (denoted by self. RB), for different average received SNR and codebook size. It is observed that at high SNR regime (20 dB), i.e. the system is cross-tier interference limited, PIC-RB outperforms self. RB. While at low SNR regime (5 dB), the two schemes share comparable performance, especially when the interference source is far away ($\delta_2 \ll 1$). To be more specific, an increasing δ_2 reflects the more dominance of the interference source, and the performance gap between PIC-RB and self. RB also gets larger. Thus, our proposed scheme is efficient for interference control. Similar observation has been made for AIC-RB scheme. Fig. 5.3 presents the achieved rate of the femtocell user with AIC-RB for different δ_1. Note that our proposed strategy is mainly aiming at controlling the cross-tier interference from the femtocell to macrocell user, at the possible rate loss for femtocell users. But, as we can see from the figure, the femtocell throughput does not degrade dramatically in comparison with the self. RB scheme, especially in the high SNR regime or δ_1 is large. Similar observation has been made for the PIC-RB scheme. Thus, our proposed coordinated beamforming design can effectively

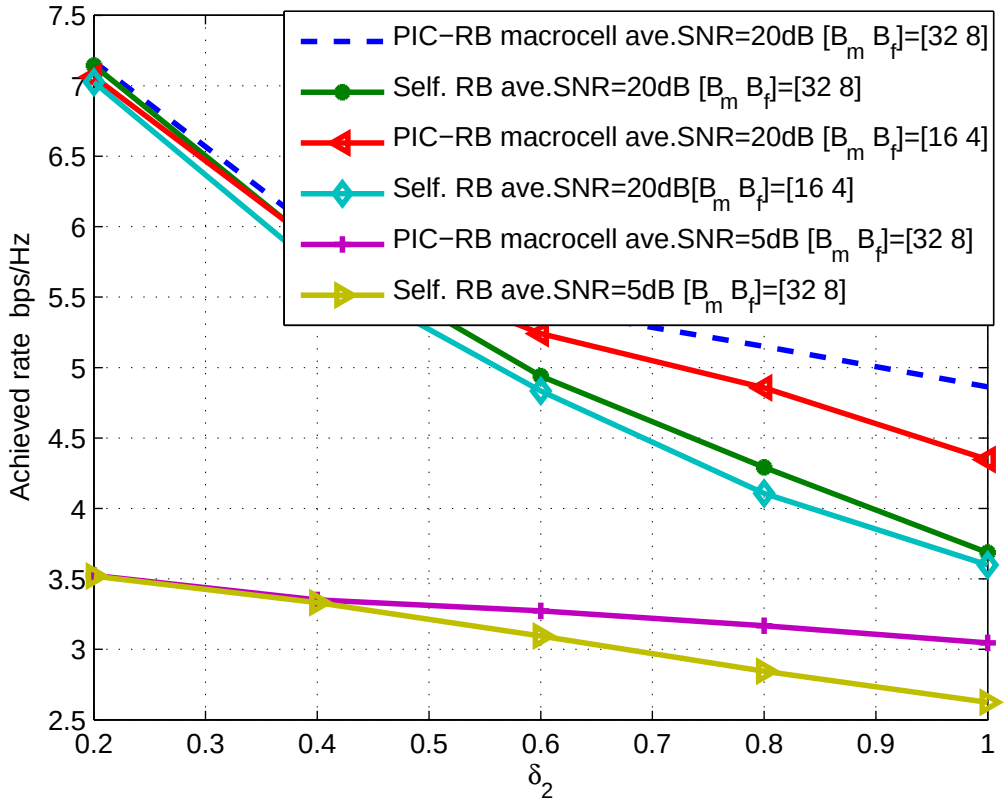

Figure 5.2: Macrocell achieved rate performance comparison ($\delta_1 = 0.5$ and $\alpha_{\mathrm{T}} = 0.4$)

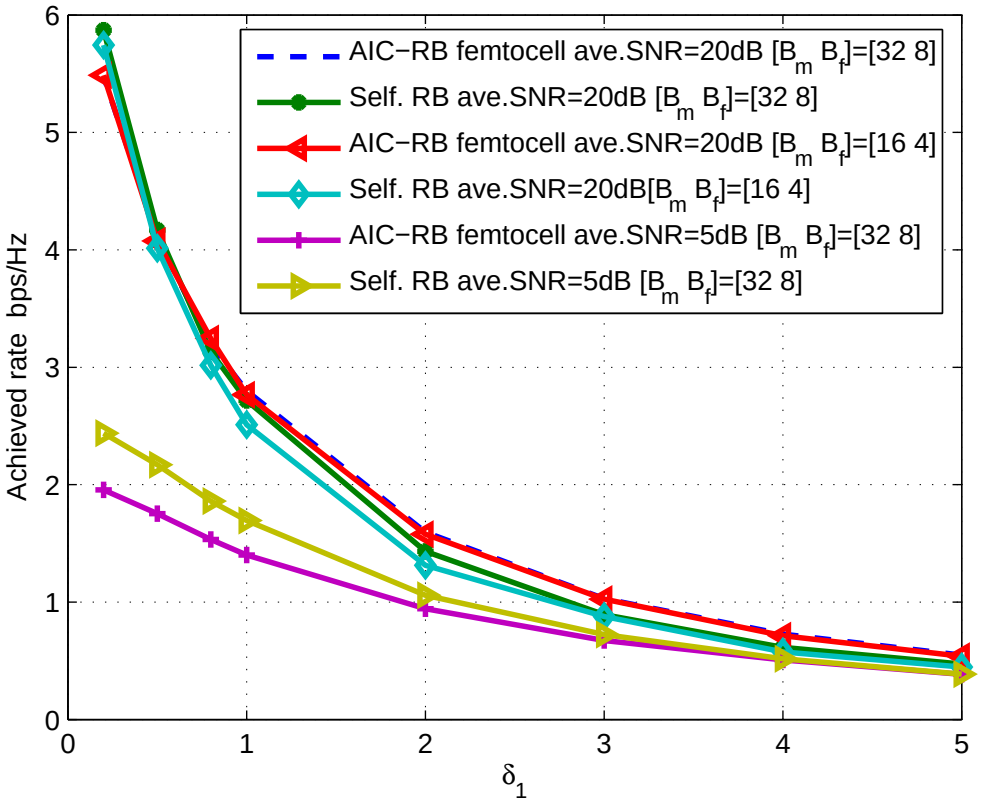

Figure 5.3: Femtocell achieved rate performance comparison ($\delta_2 = 0.7$ and $\theta_{\mathrm{T}} = 20Deg.$)

improve the overall system performance. Fig. 5.4 shows the effects of different angle thresholds θ_{T} for AIC-RB. Specifically, the sum rate for both cells is plotted as the function of θ_T. As is shown, different thresholds lead to different tradeoffs between interference tolerance and diversity gain. Specifically, if the threshold is loose, then the FAP would have more freedom to choose the best beam and its user, and vice versa. From the figure, when channel condition is poor and the system becomes noise-limited, the system inclines to make use of the more spatial degrees of freedom, while cross-tier interference is dominant, it would sacrifice the spatial freedom but to decrease the tolerance. This explains that for higher SNR, the stricter the threshold value is, the better the performance. Fig. 5.5 studies on the effect of different power thresholds α_{T} for PIC-RB. Similarly, the sum rate of both cells is plotted as the function of the normalized threshold α_{T}/E_s, where E_s denotes the symbol power. When channel condition is good, the sum rate performance reaches the peak when

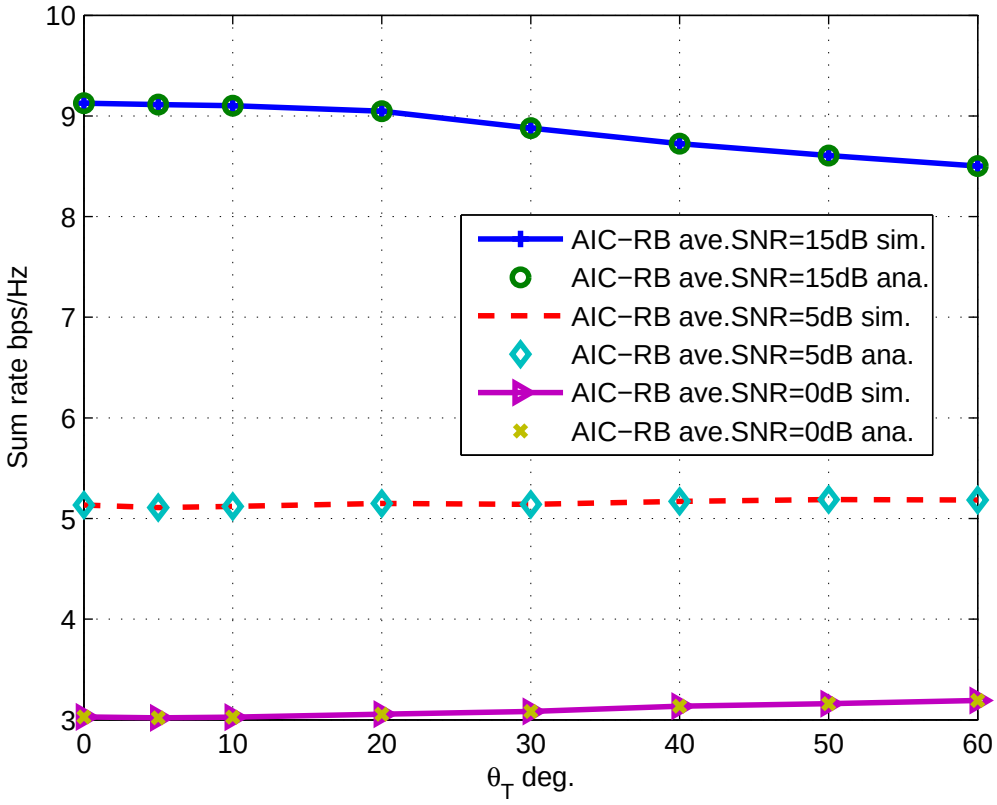

Figure 5.4: Sum rate performance comparison for AIC-RB ($\delta_1 = 0.5$ and $\delta_2 = 0.7$)

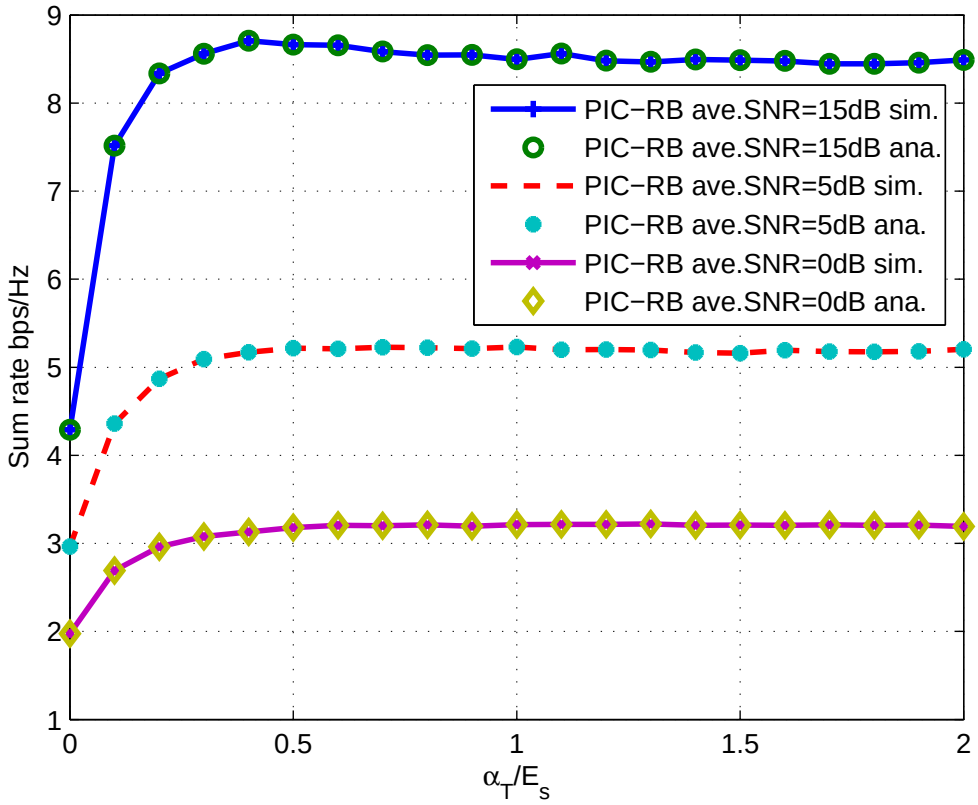

Figure 5.5: Sum rate performance comparison for PIC-RB ($\delta_1 = 0.5$ and $\delta_2 = 0.7$)

α_{T}/E_s is set to be approximately 0.4, while if the channel is poor, and the system is noise-limited, it tends to increase the threshold, so that the femtocell user can enjoy more spatial freedom. The observation is reasonable, since it reaches a good tradeoff between inter-cell interference and diversity gain. However, we also find that when α_{T}/E_s is below 0.2, the performance drops dramatically. This behavior attributes to the fact that when the threshold level is too strict, no beamforming vector can be used by FAP and, as a result, the communications in the femtocell is shut down. Finally, considering Fig. 4 and 5 together, it can be observed that when the optimal thresholds are used, the two options can provide similar sum-rate performance over low SNR region, whereas for high SNR region, AIC-RB scheme slightly outperform PIC-RB scheme.

5.5 Conclusion

In this chapter, we studied the ergodic capacity of MIMO-femtocell systems with the two proposed beamforming coordination schemes. In particular, we derived the exact analytical expressions of the ergodic sum-rate for the reduced-complexity schemes with the help of some new statistical results. We showed through selected numerical examples that our proposed coordinated beamforming schemes achieve considerable performance over conventional schemes, with only beam indexes exchange between BSs.

Chapter 6

Conclusions

In this thesis, we mainly focus on design and performance evaluation of dual-cell multiuser MIMO systems. We firstly studied the ergodic capacity of dual-cell MISO broadcast channels with low-complexity random non-orthogonal and orthogonal beamforming. Focusing on single-user scheduling in each cell, we have looked into the exact statistical derivations for the sum-rate analysis of the proposed systems, in order to reach the specific design, aiming at sum-rate maximization. We showed through selected numerical examples that our proposed schemes achieve tremendous performance over any other non-coordinated schemes for any volume of active users, with only certain beam indexes sharing between cells.

Afterwards, for multi-user scheduling per cell case, we have investigated an iterative optimization algorithm which exploits the second-order cone programming (SOCP) approaches, so as to provide an optimal performance for dual-cell transmission. A more practical multi-user scheduling scheme has been introduced and discussed later, still based on random unitary codebook, with only certain beam index sharing between two cells. Simulation verifies the priority of the proposed scheme over traditional systems. Finally, we have studied the ergodic capacity of MIMO-femtocell systems with two proposed beamforming coordination schemes. In particular, we derived the exact analytical expressions of the ergodic sum-rate for the reduced-complexity schemes with the help of some new statistical results. We showed through selected numerical examples that our proposed coordinated beamforming schemes achieve considerable performance over conventional schemes, with only beam indexes exchange between BSs.

In this thesis, we considered the significant two-cell case for analytical consistency. For future work, the general multi-cell case will be under investigation. Notice that

most of the strategies described in this thesis can be extended into general n-cell case. Nevertheless, we can observe that with the increasing number of cooperative cells, the coordination procedure becomes more complex, which would make the overall system difficult to design. On going efforts are focusing on the development of efficient user scheduling strategies in multi-cell environment.

Appendix A

SOCP reformulation of (4.6)

Revisiting (4.4), For simplisity in later calculations and presentation, we reformulate the objective function in (4.4), as:

$$\sum_{i=1}^{N} \log_2 (1 + \gamma_{1i}) + \sum_{j=1}^{N} \log_2 (1 + \gamma_{2j}) \,. \tag{1}$$

Introducing a tiny perturbation and applying Taylor quadradic approximation to the original objective function, i.e.,

$$\begin{aligned} & f(\mathbf{x}) \approx f(\mathbf{x}_0) + g(\mathbf{x}_0)^T(\mathbf{x} - \mathbf{x}_0) + \frac{1}{2}(\mathbf{x} - \mathbf{x}_0)^T H(\mathbf{x}_0)(\mathbf{x} - \mathbf{x}_0), \\ & \textit{subject to}: \quad ||\mathbf{x} - \mathbf{x}_0|| \leq \beta, \end{aligned} \tag{2}$$

where $f(\mathbf{x})$ is a smooth function, with its first-order gradient function $g(\mathbf{x})$ and second-order gradient function $H(\mathbf{x})$, we have

$$\begin{aligned}
&\sum_{i=1}^{N}\log_2\left(1+\gamma_{1i}+\Delta_{\gamma_{1i}}\right)+\sum_{j=1}^{N}\log_2\left(1+\gamma_{2j}+\Delta_{\gamma_{2j}}\right)\\
&=\sum_{i=1}^{N}\log_2\left(1+\gamma_{1i}\right)+\sum_{j=1}^{N}\log_2\left(1+\gamma_{2j}\right)+\\
&\sum_{i=1}^{N}\log_2\left(1+\frac{\Delta_{\gamma_{1i}}}{1+\gamma_{1i}}\right)+\sum_{j=1}^{N}\log_2\left(1+\frac{\Delta_{\gamma_{2j}}}{1+\gamma_{2j}}\right)\\
&\approx\sum_{i=1}^{N}\log_2\left(1+\gamma_{1i}\right)+\sum_{j=1}^{N}\log_2\left(1+\gamma_{2j}\right)-\\
&\frac{1}{2}\mathbf{x}^T\left(\sum_{i=1}^{N}\frac{\mathbf{p}_i\mathbf{p}_i^T}{(1+\gamma_{1i}^n)^2}+\sum_{j=1}^{N}\frac{\mathbf{q}_j\mathbf{q}_j^T}{(1+\gamma_{2j}^n)^2}\right)\mathbf{x}+\\
&\left(\sum_{i=1}^{N}\frac{\mathbf{p}_i^T}{(1+\gamma_{1i}^n)}+\sum_{i=1}^{N}\frac{\mathbf{q}_j^T}{(1+\gamma_{2j}^n)}\right)\mathbf{x},
\end{aligned}\tag{3}$$

with

$$\mathbf{x}=[(vec(\mathbf{W}_1)_R)^T,(vec(\mathbf{W}_1)_I)^T,(vec(\mathbf{W}_2)_R)^T,(vec(\mathbf{W}_2)_I)^T]^T,\tag{4}$$

and $\mathbf{p}_i$ is the gradient function of γ_{1i} at $_{\mathbf{x}0}$, $\mathbf{q}_j$ is the gradient function of γ_{2j} at $_{\mathbf{x}0}$, both with respect to $\mathbf{x}$. Afterwards, the crucial prblem is to obtain $\mathbf{p}_i$ and $\mathbf{q}_j$, which can be directly solved by taking derivatives of γ_{1i} and γ_{2j} with $\mathbf{x}$. Meanwhile, applying linear approximation to variables in term γ_{1i} and γ_{2j}, the approximate expressions of $\mathbf{p}_i$ and $\mathbf{q}_j$ can also be obtained. And the procedure is presented below.

Starting with the following definition and seperating the real and imaginary parts of the variables, we have,

$$\begin{aligned}
&x_i=|\mathbf{h}_{1i}^T\mathbf{w}_{1i}|^2=((\mathbf{h}_{1i}^T)_R(\mathbf{w}_{1i})_R-(\mathbf{h}_{1i}^T)_I(\mathbf{w}_{1i})_I)^2+\\
&((\mathbf{h}_{1i}^T)_R(\mathbf{w}_{1i})_I+(\mathbf{h}_{1i}^T)_I(\mathbf{w}_{1i})_R)^2,
\end{aligned}\tag{5}$$

where the subscripts R and I represents the real and imaginary parts respectively.

Then, using linear approximation, x_i^{n+1} can be rewritten as:

$$x_i^{n+1}=x_i^n+2\mathbf{a}_i^T\mathbf{x},\tag{6}$$

where

$$\mathbf{x} = [vec(\Delta_{w1})_R^T, vec(\Delta_{w1})_I^T, vec(\Delta_{w2})_R^T, vec(\Delta_{w2})_I^T]^T, \tag{7}$$

with $vec()$ denoting the vectorization of a matrix. And $\mathbf{a}^T$ can be obviously obtained, as:

$$\mathbf{a}_i^T = [|\mathbf{h}_{1i}|^2(\mathbf{w}_{1i})_R, |\mathbf{h}_{1i}|^2(\mathbf{w}_{1i})_I, \mathbf{0}_{1\times 2N}]. \tag{8}$$

Similarly, the denominator of γ_{1i} is defined as y_i, and after several steps of calculation and manipulations, y_i^{n+1} can be rewritten as:

$$y_i^{n+1} = y_i^n + 2\mathbf{b}_i^T\mathbf{x}, \tag{9}$$

where

$$\begin{aligned}\mathbf{b}_i^T = [&\sum_{k=1,k\neq i}^{N} |\mathbf{h}_{1i}|^2(\mathbf{w}_{1k})_R, \sum_{k=1,k\neq i}^{N} |\mathbf{h}_{1i}|^2(\mathbf{w}_{1k})_I,\\ &\sum_{k=1}^{N} |\mathbf{h}_{2i}|^2(\mathbf{w}_{2k})_R, \sum_{k=1}^{N} |\mathbf{h}_{2i}|^2(\mathbf{w}_{2k})_I].\end{aligned} \tag{10}$$

By defining the nominator and denominator of γ_{2j} as x_j and y_j, and applying the similar technique, the updates can be presented as:

$$x_j^{n+1} = x_j^n + 2\mathbf{c}_j^T\mathbf{x}, \tag{11}$$

$$y_j^{n+1} = y_j^n + 2\mathbf{d}_j^T\mathbf{x}. \tag{12}$$

with

$$\mathbf{c}_j^T = [\mathbf{0}_{1\times 2N}, |\mathbf{h}_{2j}|^2(\mathbf{w}_{2j})_R, |\mathbf{h}_{2j}|^2(\mathbf{w}_{2j})_I]; \tag{13}$$

$$\begin{aligned}\mathbf{d}_j^T = [&\sum_{k=1}^{N} |\mathbf{h}_{1j}|^2(\mathbf{w}_{1k})_R, \sum_{k=1}^{N} |\mathbf{h}_{1j}|^2(\mathbf{w}_{1k})_I,\\ &\sum_{k=1,k\neq j}^{N} |\mathbf{h}_{2j}|^2(\mathbf{w}_{2k})_R, \sum_{k=1,k\neq j}^{N} |\mathbf{h}_{2j}|^2(\mathbf{w}_{2k})_I].\end{aligned} \tag{14}$$

Afterwards, some further steps are operated on γ_{1i} and γ_{2j} as a whole. Applying Taylor expansion to $\gamma_{1i} = \frac{x_i}{y_i}$ (with respect to x_i and y_i) and $\gamma_{2j} = \frac{x_j}{y_j}$ (with respect

to x_j and y_j), γ_{1i}^{n+1} and γ_{2j}^{n+1} can be updated as:

$$\gamma_{1i}^{n+1} = \gamma_{1i}^{n} + \left(\frac{2}{y_i^n} \mathbf{a}_i^T - \frac{2x_i^n}{(y_i^n)^2} \mathbf{b}_i^T \right) \mathbf{x} = \gamma_{1i}^{n} + \mathbf{p}_i^T \mathbf{x}; \tag{15}$$

$$\gamma_{2j}^{n+1} = \gamma_{2j}^{n} + \left(\frac{2}{y_j^n} \mathbf{c}_j^T - \frac{2x_j^n}{(y_j^n)^2} \mathbf{d}_j^T \right) \mathbf{x} = \gamma_{2j}^{n} + \mathbf{q}_j^T \mathbf{x}. \tag{16}$$

The problem can be reformulated as a standard SOCP problem. Specifically to the constraints in (4.4), a tiny perturbation $\mathbf{x}$ is introduced, and several operations and relaxations have been performed, as

$$\begin{aligned} &\sum_{i=1}^{N} ||\mathbf{w}_{1i} + \mathbf{x}||^2 = |||[(vec(\mathbf{W}_1)_R)^T, (vec(\mathbf{W}_1)_I)^T]^T + \mathbf{A}\mathbf{x}||^2 \\ &\leq P_1, \end{aligned} \tag{17}$$

$$\begin{aligned} &\sum_{j=1}^{N} ||\mathbf{w}_{2j} + \mathbf{x}||^2 = |||[(vec(\mathbf{W}_2)_R)^T, (vec(\mathbf{W}_2)_I)^T]^T + \mathbf{B}\mathbf{x}||^2 \\ &\leq P_2, \end{aligned} \tag{18}$$

where

$$\mathbf{A}_{2N^2 \times 4N^2} = [\mathbf{I}_{2N^2 \times 2N^2}, \mathbf{0}_{2N^2 \times 2N^2}], \tag{19}$$

$$\mathbf{B}_{2N^2 \times 4N^2} = [\mathbf{0}_{2N^2 \times 2N^2}, \mathbf{I}_{2N^2 \times 2N^2}]. \tag{20}$$

Therefore, the problem can be reformulated as in (4.7).

Bibliography

[1] E. Telatar, "Capacity of multi-antenna Gaussian channels," *Eur. Trans. Telecommun.*, vol. 10, pp. 585-598, Nov. 1999.

[2] D. Tse and P. Viswanath, "Fundamentals of wireless communications," *Cambridge University Press*, 2005.

[3] G. J. Foschini and M. J. Gans, "On limits of wireless communications in a fading environment when using multiple antennas," *Wireless Pers. Commun.*, vol. 6, pp. 311-335, Mar. 1998.

[4] N. Jindal and A. Goldsmith, "Dirty paper coding vs. TDMA for MIMO broadcast channels," *Proc. IEEE Int. Conf. Commun. (ICC2004)*, Paris, France, vol. 2, pp. 682-686, Jun. 2004.

[5] G. Caire and S. Shamai, "On the achievable throughput of a multiantenna Gaussian broadcast channel," *IEEE Trans. Inf. Theory*, vol. 49, no. 7, pp. 1691-1706, Jul. 2003.

[6] M. Costa, "Writing on dirty paper," *IEEE Trans. Inform. Theory*, vol. 39, no. 3, pp. 439-411, May 1983.

[7] W. Yu and J. Cioffi, "Sum capacity of Gaussian vector broadcast channels," *IEEE Trans. Inf. Theory*, vol. 52, no. 2, pp. 754-759, Feb. 2006.

[8] S. Vishwanath, N. Jindal and A. Goldsmith, "Duality, achievable rate and sumrate capacity of Gaussian MIMO broadcast channels," *IEEE Trans. Inform. Theory*, vol. 49, no. 10, pp. 2659-2668, Oct. 2003.

[9] P. Viswanath, D. Tse and R. Laroia, "Opportunistic beamforming using dumb antennas," *IEEE Trans. Inform. Theory*, vol. 48, no. 6, 1277-1293, June 2002.

[10] Q. H. Spencer, A. L. Swindlehurst, and M. Haardt, "Zero-forcing methods for downlink spatial multiplexing in multiuser MIMO channels," *IEEE Trans. Sig. Proc.*, vol. 52, pp. 461-471, Feb. 2004.

[11] M. Sharif and B. Hassibi, "On the capacity of MIMO broadcast channels with partial side information," *IEEE Trans. Inform. Theory.*, vol. 51, no. 2, pp. 506-522, Feb. 2005.

[12] D. J. Love, R. W. Heath Jr. V. K. N. Lau, D. Gesbert, B. D. Rao, and M. Andrews, "An overview of limited feedback in wireless communication systems," *IEEE Journal on Selected Areas on Commu.*, vol. 26, no. 8, pp. 1341-1365, Oct. 2008

[13] Samsung, SNU, "Downlink MIMO for EUTRA," in 3GPP TSG RAN WG1 44/R1-060335

[14] J. G. Andrews, W. Choi, and R. W. Heath Jr. , "Overcoming interference in spatial multiplexing MIMO cellular networks," *IEEE Wireless Communications Magazine*, vol. 14, no. 6, pp. 95-104, Dec. 2007.

[15] S. Catreux, P. F. Driessen, and L. J. Greenstein, "Simulation results for an interference-limited multiple-input multiple-output cellular system," *IEEE Comm. Lett.*, vol. 4, pp. 334-336, Nov. 2000.

[16] H. Dai, A. Molisch, and H. Poor, "Downlink capacity of interference limited MIMO systems with joint detection," *IEEE Trans. Wireless Commun.*, vol. 3, no. 2, pp. 442-453, Mar. 2004.

[17] S. Shamai (Shitz), O. Somekh, and B. M. Zaidel, "Multi-cell communications: an information theoretic perspective," in *Joint Workshop on Communications and Coding (JWCC)*, Florence, Italy, Oct. 2004.

[18] S. Shamai (Shitz) and B. M. Zaidel, "Enhancing the cellular downlink capacity via co-processing at the transmitting end," in *Proc. IEEE Veh. Technol. Conf.* , Rhodes, Greece, pp. 1745-1749, May 2005.

[19] H. Zhang and H. Dai, "Cochannel interference mitigation and cooperative processing in downlink multicell multiuser MIMO networks," *EURASIP Journal on Wireless Communications and Networking*, no. 2, pp. 222-235, 4th Quarter 2004.

[20] K. Karakayali, G. J. Foschini, and R. A. Valenzuela, "Network coordination for spectrally efficient communications in cellular systems," *IEEE Wireless Communications Magazine*, vol. 13, no. 4, pp. 56-61, Aug. 2006.

[21] J. Zhang, R. Chen, J. G. Andrews, A. Ghosh, and R. W. Heath, Jr., "Networked MIMO with clustered linear precoding," *IEEE Trans. Wireless Commun.*, vol. 8, no. 4, pp. 1910-1921, Apr. 2009.

[22] O. Simeone, O. Somekh, H. V. Poor, and S. Shamai, "Downlink macrodiversity with limited backhaul capacity," *EURASIP Journal on Wireless Communications and Networking*, 2009, vol. 2009.

[23] Samsung, "Inter-cell interference mitigation through limited coordination," *3GPP TSG RAN WG1*, Jeju, Korea, Aug. 2008.

[24] F. Boccardi and H. Huang, "Zero-forcing precoding for the MIMO broadcast channel under per-antenna power constraints," in *Proc. IEEE SPAWC*, Cannes, pp. 1-5, Jul. 2006.

[25] Syed A. Jafar, S. Shamai, "Degrees of freedom region for the MIMO X channel", *IEEE Transactions on Information Theory*, vol. 54, No. 1, Jan. 2008, Pages: 151-170.

[26] J. Zhang and J. G. Andrews, "Adaptive spatial intercell interference cancellation in multicell wireless networks," submitted to *IEEE J. Select. Areas Commun. special issue on Cooperative Communications in MIMO Cellular Networks*, Sept. 2009.

[27] J. Zhu and H. -C. Yang, "Low-complexity coordinated beamforming transmission for multiuser MISO systems and its performance analysis," *Proc. of IEEE Global Communications Conference (Globecom 2010)*, Miami, FL, Dec. 2010.

[28] K. Karakayali, R. Yates, G. Foschini, and R. Valenzuela, "Optimum zero-forcing beamforming with per-antenna power constraints," in *Proc. IEEE Int. Symp. Information Theory*, Nice, France, pp. 101-105, Jun. 2007.

[29] W. Yu and T. Lan, "Transmitter optimization for the multi-antenna downlink with per-antenna power constraints," *IEEE Trans. Signal Processing*, vol. 55, no. 6, pp. 2646-2660, Jun. 2007.

[30] S. A. Jafar, G. Foschini, and A. J. Goldsmith, "Phantomnet: Exploring optimal multicellular multiple antenna systems," *EURASIP Journal on IIN-Appl. Signal Processing, Special issue on MIMO Comm. and Signal Processing*, pp. 591-605, May 2004.

[31] K. Karakayali, G. J. Foschini, and R. A. Valenzuela, "Network coordination for spectrally efficient communications in cellular systems," *IEEE Wireless Communications Magazine*, vol. 13, no. 4, pp. 56-61, Aug. 2006.

[32] G. J. Foschini, K. Karakayali, and R. A. Valenzuela, "Coordinating multiple antenna cellular networks to achieve enormous spectral efficiency," *IEE Proceedings*, vol. 153, no. 4, pp. 548-555, Aug. 2006.

[33] H. Huang and S. Venkatesan, "Asymptotic downlink capacity of coordinated cellular network," in *Proc. of the IEEE Asilomar Conf. on Signals, Systems, and Computers*, Pacific Grove, CA, pp. 850-855, Nov. 2004.

[34] D. Aktas, M. N. Bacha, J. S. Evans, and S. V. Hanly, "Scaling results on the sum capacity of cellular networks with MIMO links," *IEEE Trans. Inform. Theory*, vol. 52, no. 7, pp. 3264-3274, Jul. 2006.

[35] S. Jing, D. N. C. Tse, J. Hou, J. B. Soriaga, J. E. Smee, and R. Padovani, "Multi-cell downlink capacity with coordinated processing," *EURASIP Journal on Wireless Communications and Networking*, 2008, vol. 2008, Article IE 586878.

[36] Samsung, "Inter-Cell Interference Mitigation Through Limited Coordination," *3GPP TSG RAN WG1*, Jeju, Korea, Aug. 2008.

[37] V. Chandrasekhar, J. Andrews, and A. Gatherer, "Femtocell Networks: A Survey," *IEEE Communications Magazine*, vol. 46, no. 9, pp. 59-67, Sept. 2008.

[38] Tropos Networks, "Picocell mesh: Bringing low-cost coverage, capacity and symmetry to mobile WIMAX,", White paper.

[39] V. Chandrasekhar, J. Andrews, T. Muharemovic, Z. Shen and A. Gatherer, "Power control in two-tier femtocell networks," *IEEE Transactions on Wireless Communications*, vol. 8, no. 8, pp. 4316-4328, Aug. 2009.

[40] V. Chandrasekhar and J. G. Andrews, "Uplink capacity and interference avoidance for two-tier femtocell networks", *IEEE Transactions on Wireless Communications*, vol. 8, no. 7, pp. 3498-3509, July 2009.

[41] J.-S. Wu, J.-K. Chung, and Y.-C. Yang, "Performance study for a microcell hot spot embedded in CDMA macrocell systems", *IEEE Trans. on Veh. Techno.*, vol. 48, no. 1, pp. 47-59, Jan. 1999.

[42] H. -S. Jo, C. Mun and J. -G. Yook, "Interference mitigation using uplink power control for two-tier femtocell networks," *IEEE Transactions on Wireless Communications*, vol. 8, no. 10, pp. 4906-4910, Oct. 2009.

[43] S. Park, W. Seo, Y. Kim, S. Lim and D. Hong, "Beam subset selection strategy for interference reduction in two-tier femtocell networks," *IEEE Transactions on Wireless Communications*, vol. 9, no. 11, pp. 3440-3449, Nov. 2010.

[44] Alcatel-Lucent, "UE PMI feedback signalling for user pairing/coordination," *3GPP TSG RAN WG1*, Prague, Czech Republic, Sept. 2008.

[45] A. G. Glen, L. M. Leemis and J. H. Drew, "Computing the distribution of the product of the two continuous random variables," *ELSEVIER Computational Statistics and Data Analysis*, Vol. 44, no. 3, pp. 451-464, Jan. 2004.

[46] R. Chen, R. W. Heath Jr., and J. G. Andrews, "Transmit selection diversity for unitary precoded multiuser spatial multiplexing systems with linear receivers," *IEEE Trans. on Signal Processing*, Mar. 2007.

[47] Z. Shen, R. Chen, J. G. Andrews, R. W. Heath Jr., and B. L Evans, "Low complexity user selection algorithms for multiuser MIMO systems with block diagonalization," *IEEE Trans. on Signal Processing*, vol. 54, no. 9, pp. 3658C3663, Sep. 2006.

[48] O. Somekh, B. Zaidel and S. Shamai (Shitz), "Sum rate characterization of joint multiple cell-site processing", *IEEE Trans. on Inform. Theory*, vol. 53, no. 12, pp. 4473- 4497, Dec. 2007.

[49] S. Shim, J. S. Kwak, R. W. Heath Jr. and J. G. Andrews, "Downlink MIMO block diagonalization in the presence of other-cell interference," *Proceedings of IEEE Global Communications Conference 2007 (Globecom'07)*, pp. 4354- 4358, Washington DC, Nov. 2007.

[50] H. Dahrouj, and W. Yu: "Coordinated beamforming for the multicell multi-antenna wireless systems," *IEEE Transactions on Wireless Communications*, vol. 9, no. 5, pp. 1748-1795, May 2010.

[51] B. Hassibi and T. L. Marzetta, "Multiple-antennas and isotropically random unitary inputs: the received signal density in closed form," *IEEE Trans. Inform. Theory*, vol. 48, no. 6, pp. 1473-1484, June 2002.

[52] M. Sharif, and B. Hassibi, "On the capacity of MIMO broadcast channels with partial side information," *IEEE Trans. Inform. Theory*, vol. 51, no. 2, pp. 506-522, Feb. 2005.

[53] A. Antoniou and W.-S. Lu, "Practical optimization: algorithms and engineering applications," *Springer*, New York, NY, 2007.

[54] 3GPP TSG RAN WG1 31 R1-030354, Per unitary basis stream user and rate control (PU2RC), *3GPP TSG-R1-030354*, Tokyo, Fed 18-21, 2003. (See also R1-030130)

[55] S. J. Kim, H. J. Kim, C. S. Park, and K. B. Lee, "On the performance of multiuser MIMO systems in WCDMA/HSDPA: beamforming, feedback and user diversity," *IEICE Transactions on Communications*, vol. E98-B, no. 8, pp. 2161C2169, Aug. 2006.